

Research article

Integrating network pharmacology and experimental verification to decipher the multitarget pharmacological mechanism of *Cinnamomum zeylanicum* essential oil in treating inflammation

Debajani Mohanty, Sucheesmita Padhee, Chiranjibi Sahoo, Sudipta Jena, Ambika Sahoo, Pratap Chandra Panda, Sanghamitra Nayak, Asit Ray*

Centre for Biotechnology, Siksha O Anusandhan (Deemed to be University), Kalinganagar, Ghatikia, Bhubaneswar-751003, Odisha, India

ARTICLE INFO

Keywords:

Anti-inflammatory
Cinnamomum zeylanicum bark essential oil
Molecular docking
Network pharmacology
RAW 264.7 cells

ABSTRACT

Inflammatory diseases contribute to more than 50 % of global deaths. Research suggests that network pharmacology can reveal the biological mechanisms underlying inflammatory diseases and drug effects at the molecular level. The aim of the study was to clarify the biological mechanism of *Cinnamomum zeylanicum* essential oil (CZEO) and predict molecular targets of CZEO against inflammation by employing network pharmacology and *in vitro* assays. First, the genes related to inflammation were identified from the Genecards and Online Mendelian Inheritance in Man (OMIM) databases. The CZEO targets were obtained from the SwissTargetPrediction and Similarity Ensemble Approach (SEA) database. A total of 1057 CZEO and 526 anti-inflammation targets were obtained. The core hub target of CZEO anti-inflammatory was obtained using the protein–protein interaction network. KEGG pathway analysis suggested CZEO to exert anti-inflammatory effect mainly through Tumor necrosis factor, Toll-like receptor and IL-17 signalling pathway. Molecular docking of active ingredients-core targets interactions was modelled using Pyrx software. Docking and simulation studies revealed benzyl benzoate to exhibit good binding affinity towards IL8 protein. MTT assay revealed CZEO to have non-cytotoxic effect on RAW 264.7 cells. CZEO also inhibited the production of NO, PGE₂, IL-6, IL-1 β and TNF- α and promoted the activity of endogenous antioxidant enzymes in LPS-stimulated RAW 264.7 cells. Additionally, CZEO inhibited intracellular ROS generation, NF- κ B nuclear translocation and modulated the expression of downstream genes involved in Toll-like receptor signalling pathway. The results deciphered the mechanism of CZEO in treating inflammation and provided a theoretical basis for its clinical application.

1. Introduction

Inflammatory diseases such as cancer, diabetes mellitus, chronic kidney disease, and stroke contribute to more than 50 % of global deaths [1]. Inflammation is a highly-regulated cascade of events initiated by physical, chemical and biological stimuli and provides a defence to the host by resolving the infection [2,3]. Although self-limiting inflammation is physiological and essential for pathogen elimination, its persistence harms the infected organs and leads to chronic diseases [4,5]. An unresolved inflammatory response

* Corresponding author.

E-mail address: asitray@soa.ac.in (A. Ray).

<https://doi.org/10.1016/j.heliyon.2024.e24120>

Received 1 July 2023; Received in revised form 3 January 2024; Accepted 3 January 2024

Available online 10 January 2024

2405-8440/© 2024 The Author(s). Published by Elsevier Ltd. This is an open access article under the CC BY-NC-ND license (<http://creativecommons.org/licenses/by-nc-nd/4.0/>).

disturbs the immune homeostasis of the host cell. Therefore, a delicate balance must be maintained between pro-inflammatory and anti-inflammatory cytokine levels [6]. Reduction in expression of pro-inflammatory mediators can alleviate the severity of chronic inflammation [7]. During inflammatory disease, macrophages release excess mediators and activate pro-inflammatory downstream signal transduction pathway [8]. LPS-activated macrophage results in the release of nitric oxide (NO), interleukin (IL)-6, interleukin (IL)-1 β and tumor necrosis factor (TNF)- α via NF- κ B signalling pathway [9,10]. As a result, LPS-treated RAW 264.7 cells can be used as an *in vitro* model to understand the mechanism of anti-inflammatory agents.

Non-steroidal anti-inflammatory drugs (NSAIDs) are used to treat inflammation, inhibiting the synthesis of prostaglandin by blocking the activity of cyclooxygenase enzymes [11]. However, prolonged consumption of these NSAIDs is known to cause adverse health complications such as renal, bone, gastrointestinal tract and cardiovascular problems [12]. In recent years, there has been growing evidence that herbal medicines significantly lower inflammation [13]. Therefore, there is a global demand to search for safe and effective phytochemicals with fewer side effects.

The genus *Cinnamomum* of the family Lauraceae comprises nearly 200 species, among which 20 species occur in India [14]. *Cinnamomum zeylanicum* Blume, an important member of genus *Cinnamomum* is native to Sri Lanka, Myanmar and South East Asia [15, 16]. The bark of *C. zeylanicum* is used as a potent therapeutic agent in the Ayurvedic system of medicine for treating several ailments, including arthralgia, myalgia, digestive, gynaecology and respiratory disorders [17]. *C. zeylanicum* essential oil extracted from the bark exhibited several efficacies such as anti-inflammatory, anti-diabetic, antioxidant, anti-microbial properties [18].

Former *in vivo* study showed that nano gel-formulation of *C. zeylanicum* essential oil possess substantial anti-inflammatory property in carrageenan-induced paw edema in rats [19]. *In vitro* study on commercially available *C. zeylanicum* bark essential oil exhibited anti-inflammatory effects in human skin disease models [18]. Although there are claims on the anti-inflammatory property of *C. zeylanicum* essential oil, the underlying mechanism behind its anti-inflammatory action is still unclear. Therefore, identifying potential active compounds and therapeutic targets will improve the understanding of the anti-inflammatory mechanism of *C. zeylanicum* essential oil.

Bioinformatics approaches have been used to systematically reveal the biological mechanisms underlying complex diseases and drug effects at the molecular level. Network pharmacology has been proven to be an emerging approach for identifying the potential molecular targets and their fundamental mechanism from a comprehensive and holistic viewpoint [20,21]. Therefore, in the current research network pharmacology was conducted to establish the components-targets-pathways-disease network and to investigate the potential mechanisms of CZEO in treating inflammation. Additionally, molecular docking and simulation approaches further validated the binding of the potential bioactive constituents and core inflammatory targets. Then, the pathways suggested by network pharmacology were validated using LPS-induced RAW 264.7 inflammation model. The schematic workflow of the study is illustrated in Fig. 1.

2. Materials and methods

2.1. Plant material and extraction of essential oil

Fresh bark of *Cinnamomum zeylanicum* was collected from medicinal plant garden of Institute of Mineral and Material Technology, Bhubaneswar, Odisha, India. The identification of this species was confirmed by Dr. P.C. Panda, Professor, Center of Biotechnology, SOA University, Odisha, India. The voucher specimen (2452/CBT Dt. November 10, 2022) was deposited in the Herbarium of Centre of Biotechnology, SOA University, Bhubaneswar. The bark was dried under shade at room temperature, grounded and then passed through a 60-mesh sieve. Essential oil from dried bark (200 g) was extracted by hydrodistillation using Clevenger apparatus for 6 h according to the method described in European Pharmacopoeia [22]. Anhydrous sodium sulphate was added to essential oil to remove the traces of water.

2.2. Chemical characterization of essential oil

The essential oil was characterized using Clarus 580 GC (PerkinElmer, USA) fitted with an SQ-8 MS detector. 0.1 μ l of essential oil was injected into the system in splitless mode. Compounds separation was done using helium (1 ml/min) as carrier gas on an Elite-5 MS capillary column (30 m, 0.25 mm i.d., 0.25 μ m thickness). The temperature was set at 60 $^{\circ}$ C, raised to 220 $^{\circ}$ C at a rate of 3 $^{\circ}$ C/min, and maintained there for 7 min. The ion source and detector temperature was set at 250 $^{\circ}$ C and 150 $^{\circ}$ C, respectively. The electron ionization energy was set at 70 eV. Individual constituents of essential oil were determined based on RI (Retention Index), which was evaluated using n-alkane series (C₈–C₂₀) on Elite-5 MS capillary column run under identical operating condition. Compound identification was performed by matching their recorded mass-spectra with the mass spectra of the inbuilt National Institute of Standards and Technology (NIST) library provided in the system. Additional comparison was done by checking the experimental retention indices values obtained with those published in the literature [23].

2.3. Network pharmacology

2.3.1. Prediction of bioactive constituents

All the phytoconstituents obtained from GC-MS analysis were subjected for pharmacokinetic screening in Swiss ADME online web tool (<http://www.swissadme.ch/>). The screening criteria were set as Lipinski's rule and the abbot oral bioavailability (OB) value \geq 0.5. The constituents which qualified both the parameters were considered as active constituents.

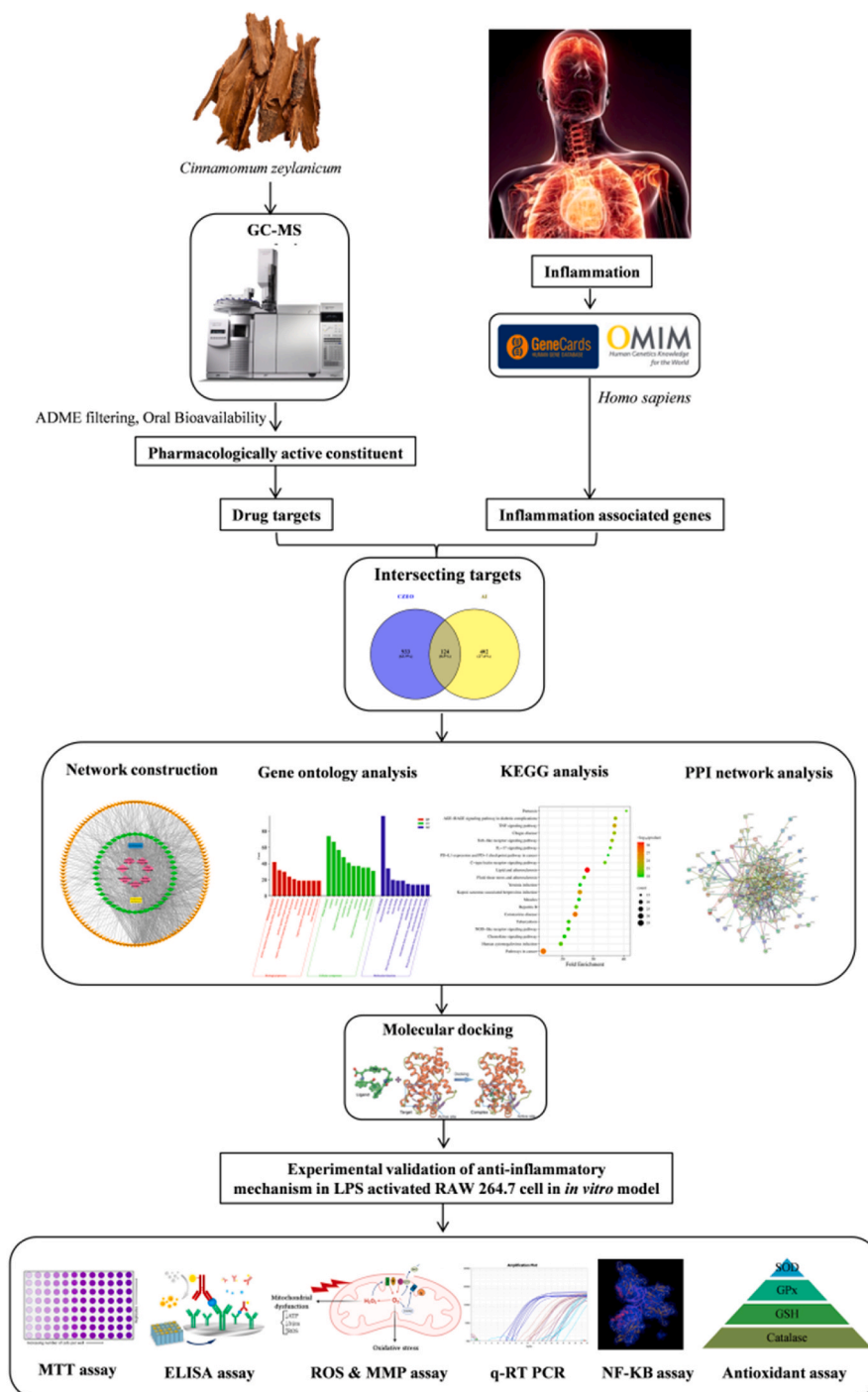


Fig. 1. Schematic flowchart of the proposed work.

2.3.2. Acquisition of compound and inflammation-associated targets

The predicted targets of screened bioactive compounds were done by putting the SMILES into Swiss Target Prediction (STP) (<http://www.swisstargetprediction.ch/>) and Similarity Ensemble Approach (<https://sea.bkslab.org/>). Inflammation-related genes were acquired from Online Mendelian Inheritance in Man (OMIM) (<https://omim.org/>) and Gene Cards (<https://www.genecards.org/>) by entering the keyword 'anti-inflammation'. Venny 2.1.0 (<https://bioinfoq.cnbc.csic.es/tools/venny/>) online platform was used to ascertain the genes shared by both CZEO targets and inflammation targets. These intersecting genes were considered as CZEO target genes involved in treating inflammation.

2.3.3. Compound-target disease network construction

Compound-target-disease network was created to analyse and visualize the interrelationship between phytoconstituents, targets and disease-related pathways using Cytoscape 3.9.1 software [24]. For visualisation, potential active components and targets of CZEO were imported into Cytoscape 3.9.1 software, and a network of CZEO components and anti-inflammatory targets was built. In the compound-target network, each component or target is represented by a node, and the relationship between the component and the target is represented by a connecting line. The degree value reflects the importance of the node in the network; the higher the value, the more important the node. And the core active ingredients were screened out by the degree values.

2.3.4. Protein-protein interaction (PPI) analysis

The key target genes obtained from the intersection of two gene datasets were enriched in the STRING database (<https://string-db.org/>) to get a PPI network containing both direct and indirect connections among proteins. The screening criteria in the STRING database was limited to species *Homo sapiens* and confidence score was set to >0.7. Cytohubba module of Cytoscape was used to screen and visualize the densely linked protein based on degree algorithm [25]. These genes were considered hub targets for the treatment of inflammation.

2.3.5. GO and KEGG enrichment analysis

The functional enrichment analysis of intersecting therapeutic targets were assessed based on Kyoto Encyclopaedia of Genes and Genomes (KEGG) and Gene Ontology (GO). GO enrichment analysis discloses the biological mechanism associated with key therapeutic targets. KEGG enrichment analysis depicts the functional pathways annotations of key targets. Three GO terms (biological function, molecular function and cellular component) were analyzed in DAVID database (<https://david.ncicrf.gov/>) and visualisation was done in SRPLOT (<https://www.bioinformatics.com.cn/en>). KEGG pathway enrichment analysis was performed in ShinyGO 0.77 (<http://bioinformatics.sdstate.edu/go/>) database and visualisation was also done in SRPLOT. The cut-off value for significant KEGG pathway enrichment analysis was set as $p < 0.05$ and $FDR < 0.01$. The KEGG mapper (<http://www.kegg.jp.org/>) highlighted the top pathway and demonstrated its distinct molecular mechanism within that particular pathway.

2.3.6. Molecular docking

Molecular docking simulation provides an in-depth understanding of the binding mechanism between targeted protein and probable drug ligands. Initially the hub genes were searched in the UniProt database (<https://www.uniprot.org/>) to validate this. The crystal structures of hub target proteins were: TNF (PDB ID: 2AZ5), IL6 (PDB ID:1ALU), TLR4 (PDB ID: 2Z63), STAT3 (PDB ID: 6NJS), IL8 (PDB ID: 6N2U) and NFKB (PDB ID: 1NFI), and were downloaded from RCSB Protein Data Bank (<http://www.rcsb.org/pdb>) in PDB format. Three dimensional structures of protein targets were modelled by eliminating water, ligands, ions, heteroatoms from atoms, and adding polar hydrogen atom, gasteiger and kollman charges to protein structure. SDF formats of ligands (Hydrocinnamyl acetate, benzyl benzoate, ethyl cinnamate, benzyl cinnamate, cinnamic acid, α -muurolene and hexadecanoic acid) were obtained from Pubchem database (<https://pubchem.ncbi.nlm.nih.gov/>) and discovery visualizer was utilized for converting the SDF files into PDB files. Molecular docking between bioactive constituents (ligands) and refined protein targets was performed using the Autodock vina plugin tool of PyRx software. Energy minimization of compounds were done in PyRx. The PDB files of protein and ligand were converted into their PDBQT format in Auto Dock Tool. Complete protein was covered under grid box and docking was done with all default parameter settings. The validation of docking was confirmed based on low RMSD (<2 Å) of the redocked ligand from the orientation of the cocrystallized ligand and the reproduction of observed interactions from the pdb structure. The BIOVIA Discovery Studio visualizer tool was used to visualize the best-docking poses.

2.3.7. Molecular dynamics

Molecular dynamics simulation was carried out using the Schrodinger software's Desmond module. In MD simulation, an orthorhombic box was generated with simple point charge (SPC) solvent model system of water. The salt concentration was kept constant at 0.15 M, and the model was optimized. The MD simulation was performed using a constant temperature and pressure (NPT) at 310 K and 1.013 bar atmospheric pressure for 100 ns. A total of 1000 frames were generated during the simulation. The outcome of the simulation results was examined by calculating the root mean square deviation, root means square fluctuation, and ligand interaction profile obtained using the simulation interaction diagram report.

2.4. Experimental assays

2.4.1. Cell culture

RAW 264.7 cells were purchased from NCCS, Pune, India. The cells were cultured in DMEM (Dulbecco's Modified Eagle Medium) high glucose media, enriched with 10 % Fetal Bovine Serum (FBS), 1 % L-Glutamine (200 mM) and 1 % antibiotic-antimycotic solution. RAW 264.7 cells were maintained in a humidified incubator containing 5 % CO₂ and 18–20 % O₂ at 37 °C.

2.4.2. Cytotoxicity assay

The cytotoxic effect of CZEO on RAW 264.7 cells were assessed using MTT assay. Essential oils of *Cinnamomum zeylanicum* were prepared by dissolving them in 0.5 % (v/v) DMSO. Initially, RAW 264.7 cells were incubated in 96-well plate (1×10^5 cells/ml) and allowed to grow for 24 h in a CO₂ incubator. Cells were treated with different essential oil concentrations (12.5–100 µg/ml) and incubated for another 24 h. After 24 h, the used media was removed and MTT reagent (50 µg/ml) was added. The produced formazan

crystals were solubilized by adding DMSO. Then absorbance of this solution was taken by an ELISA plate reader at 570 nm.

2.4.3. Nitric oxide assay

RAW 264.7 cells (1×10^5 cells/ml) were seeded in a culture plate and incubated for 24 h. Then the cells were pre-incubated with LPS (1 $\mu\text{g/ml}$) except in untreated well. Cells were then exposed to different concentrations of essential oil (12.5 and 100 $\mu\text{g/ml}$) and incubated at 37 °C in a humidified incubator for 24 h. Then Griess reagent (100 μl) was mixed with 100 μl of culture supernatant. Then the solution was kept at 37 °C for 2 h and absorbance was measured at 540 nm using Microplate reader (ELX 800, BioTek, USA). The quantification was done on the basis of sodium nitrite standard curve.

2.4.4. Measurement of prostaglandin- E_2 (PGE $_2$) levels

RAW 264.7 cells (1×10^5 cells/ml) were seeded in culture plate and incubated at 37 °C for 24 h for cell fixation and to achieve desired cell density. Then, the cells were stimulated with LPS (1 $\mu\text{g/ml}$) for 2 h followed by exposure to different concentrations of CZEO (12.5 and 100 $\mu\text{g/ml}$) and incubated for another 24 h. After incubation, supernatants were collected. The level of PGE $_2$ was determined using enzyme immunoassay (EIA) following the supplier's instructions (Cayman Chem, Ann Arbor, Michigan, USA). Then Ellman's reagent was added and the colour intensity was measured by taking the absorbance at 405 nm.

2.4.5. Measurement of TNF- α , IL6 and IL-1 β levels

RAW 264.7 cells at a density of 1×10^5 cells/ml were plated and incubated for 24 h for cell adhesion and to achieve the required cell density. Cells were stimulated with LPS (1 $\mu\text{g/ml}$) followed by treatment in the absence or presence of CZEO (12.5 and 100 $\mu\text{g/ml}$) and kept in humidified atmosphere for 24 h. After incubation, the culture media were centrifuged. After centrifugation, supernatants were collected to estimate the levels of IL-6, IL-1 β and TNF- α . Quantification of pro-inflammatory cytokines was measured by quantitative ELISA using the kits obtained from RayBiotech Laboratories (Norcross, GA).

2.4.6. Measurement of endogenous antioxidant enzymes

RAW 264.7 cells (1×10^5 cells/ml) were grown in a culture dish and incubated for 24 h in a humidified incubator for cell attachment and to achieve the required cell density. Then cells were stimulated with 1 $\mu\text{g/ml}$ of LPS and incubated for another 2 h to induce inflammation. Subsequently, cells were incubated with different concentrations of CZEO (12.5 and 100 $\mu\text{g/ml}$) for 24 h. Cells were harvested, sonicated and centrifuged to get the cell lysate. Antioxidant enzymes including superoxide dismutase (SOD), glutathione (GSH), glutathione peroxidase (GPx) and catalase (CAT) were assessed from cell free supernatant by following the instruction mentioned in the kit (Krishgen Biosystems, Mumbai, India).

2.4.7. Measurement of intracellular reactive oxygen species

The production of intracellular reactive oxygen species (ROS) in RAW 264.7 cells was measured using 2',7'-dichlorodihydrofluorescein diacetate (DCFH-DA) assay. Briefly, RAW 264.7 cells (1×10^5 cells/ml) were seeded in the culture dish and treated with LPS (1 $\mu\text{g/ml}$) followed by incubation with varying concentration of CZEO (12.5 and 100 $\mu\text{g/ml}$) for 24 h in a humidified atmosphere. After 24 h of incubation, cells were exposed to DCFH-DA for 30 min. Thereafter media was discarded and the cells were washed twice with cold PBS followed by centrifugation. Then the cell pellets were suspended in DMSO and the level of reactive oxygen species was visualized under a fluorescent microscope.

2.4.8. Measurement of mitochondrial membrane potential

RAW 264.7 cells (1×10^5 cells/ml) were grown in a culture dish for 24 h. Mitochondrial membrane potential in RAW 264.7 cells was assessed using JC-1 dye. Initially cells were treated with LPS (1 $\mu\text{g/ml}$) followed by treatment with different doses of CZEO (12.5 and 100 $\mu\text{g/ml}$) and was incubated for another 24 h. Then the cells were rinsed with PBS, stained with 1 $\mu\text{g/ml}$ of JC-1 dye for 30 min and kept at 37 °C. Then the cells were observed under a fluorescent microscope.

2.4.9. NF- κ B nuclear translocation

RAW 264.7 cells (1×10^5 cells/ml) were plated in well plate and incubated in 5 % CO $_2$ incubator for 24 h. Cells were induced with LPS (1 $\mu\text{g/ml}$) except in untreated well and kept for 2 h before CZEO treatment. Then the cells were treated with the required concentrations of CZEO and incubated for another 24 h in a humidified incubator. After incubation, the culture media were removed and rinsed with PBS. Following this, 0.5 ml of BD Cytofix/Cytoperm solution was added. Then the cells were washed and immune stained with 10 μl of PE Mouse anti-NF κ B p65 antibody, followed by counterstaining with 100 μl of 1 $\mu\text{g/ml}$ DAPI solution. Cells were visualized under the confocal laser scanning microscope ZEISS LSM 880 (Carl Zeiss, Oberkochen, Germany) and expression of NF κ B-p65 was measured in Image J software.

2.4.10. RNA extraction and reverse transcriptase quantitative polymerase chain reaction (RT-qPCR) analysis

RAW 264.7 cells were seeded as described above. The cells were exposed to LPS (1 $\mu\text{g/ml}$) to induce inflammation, followed by treatment with varying concentrations of CZEO (12.5 and 100 $\mu\text{g/ml}$) and incubated for 24 h. The RNA extraction was performed using RNeasy kit (Qiagen, Chatsworth, CA, USA) and synthesis of cDNA was performed using the iScript cDNA synthesis kit (Bio-Rad Laboratories, Hercules, CA, USA). The expression analysis was done in Qiagen RotorGene Q 5 plex HRM using the SYBR Green. The PCR conditions were set to 40 cycles and the reaction conditions were as follows: initial denaturation at 95 °C for 5 min, denaturation at 95 °C for 10 s, annealing at 60 °C for 20 s and extension at 72 °C for 20 s. Each gene relative expression was calculated using $2^{-\Delta\Delta Ct}$

method compared to β -actin. The primers sequence used are listed in Table 1.

2.5. Statistical analysis

The data obtained are mean \pm SD of three independent experiments. Statistical significance analysis was performed using analysis of variance (ANOVA) followed by Tukey's test using GraphPad Prism software.

3. Results

3.1. Chemical constituents of CZEO by GC-MS

The bark essential oil of *Cinnamomum zeylanicum* (CZEO) was pale yellow with an oil yield of 0.4 (%v/w) on a dry weight basis. A total of 57 constituents were detected, accounting for 95.54 % of total bark oil (Table 2). The major compounds were (*E*)-Cinnamaldehyde (33.31 %), Eugenol (11.37 %), Benzyl benzoate (11.22 %), Camphor (7.96 %) and Linalool (4.72 %) (Fig. 2). The phytoconstituents of CZEO were classified broadly into eight groups such as phenylpropanoids (46.88 %) followed by oxygenated monoterpenes (19.07 %), benzenoids (14.34 %), oxygenated sesquiterpenes (7.09 %), monoterpene hydrocarbons (3.63 %), sesquiterpene hydrocarbons (3.58 %), oxygenated diterpene (0.19 %) and others (0.76 %).

3.2. Screening of bioactive constituents and acquisition of compound and inflammation-related targets

The chemical constituents identified by GC-MS were screened for their drug-likeness properties by following Lipinski's rule and Abbott Bioavailability score. Lipinski's rule states that the molecular weight of a compound should be less than 500 amu, H-bond donor should be less than 10, H-bond acceptor should be less than 5, lipophilicity value should be less than 5. Abbott bioavailability score should be greater than 0.5 for an orally active drug. Out of 57 constituents identified from GC-MS analysis, 52 were screened as bioactive constituents as they passed the above criteria (Table 3). Then, the bioactive constituents were subjected to acquire compound targets from public databases. A total of 1057 predicted targets for CZEO were identified by Swiss Target Prediction (STP) and Similarity Ensemble Approach (SEA) database, respectively. The Venn diagram-based analysis revealed the presence of 335 common targets between STP and SEA database. A total of 488 and 284 targets were screened from Genecards (targets with relevance score >10 were only included) and OMIM database, respectively. 246 intersectional targets were obtained. Subsequently, 526 targets were considered as anti inflammation-related therapeutic targets. Thereafter, compound-disease intersecting targets were obtained by intersecting compound targets and disease targets genes using Venny 2.1.0 online tool. A total of 124 common intersecting targets were obtained (Fig. 3A).

3.3. Compound target network analysis


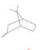
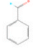

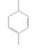
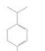
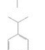
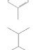
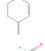
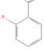
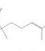



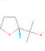

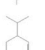
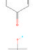
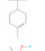
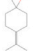



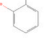
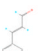
Cytoscape 3.9.1 software was used to visualize and correlate the interlink between compounds and targets used in treating inflammation by constructing a compound-target disease network. The network consists of 177 nodes interacting through 1125 edges (Fig. 3B). This pharmacological network indicates that one compound can target multiple genes. In order to determine the significant key components among the detected constituents, constituents were filtered on the basis of the degree value. Seven hub compounds were selected based on their degree value, including hydrocinnamyl acetate (degree-50), benzyl benzoate (degree-50), ethyl cinnamate (degree-44), benzyl cinnamate (degree-37), cinnamic acid (degree-32), α -muurolene (degree-31) and hexadecanoic acid (degree-31) (Table 4).

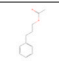
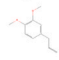
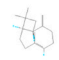
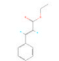
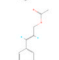
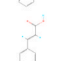
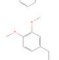
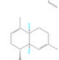
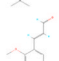
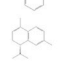
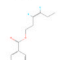
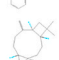
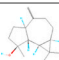

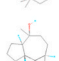
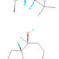
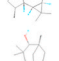
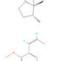
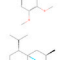
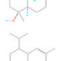
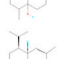
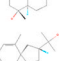
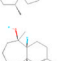
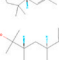
Table 1
Primer sequences used for qRT-PCR analysis.

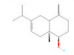
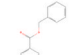
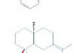
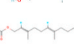

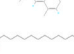
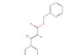

Gene	Primer	Sequence (5'-3')
β -actin	Forward	CATTGCTGACAGGATGCAGAAGG
	Reverse	TGCTGGAAGGTGGACAGTGAGG
TLR4	Forward	CCCTGAGGCATTTAGGCAGCTA
	Reverse	AGGTAGAGAGGTGGCTTAGGCT
IL8	Forward	GAGAGTGATTGAGAGTGACCCAC
	Reverse	CACAACCCTCTGCACCCAGTTT
IL6	Forward	AGACAGCCACTCACCTCTTCAG
	Reverse	TTCTGCCAGTGCCCTCTTGCTG
NF κ B	Forward	GCAGCACTACTTCTTGACCACC
	Reverse	TCTGCTCCTGAGCATTGACGTC
TNF	Forward	CTCTCTGCCTGCTGCACTTTG
	Reverse	ATGGGCTACAGGCTTGTCACTC

Table 2

Chemical characterization of *Cinnamomum zeylanicum* bark essential oil RI_{exp}: Retention indices calculated on the basis of homologous n-alkane series (C₈–C₂₀) on an Elite-5 MS column. RI_{lit}: Retention indices published in literature (Adams, 2007).

No.	Compounds	RI _{exp}	RI _{lit}	Peak Area%	2D structure
1	α -Thujene	928	930	0.26	
2	α -Fenchene	944	952	0.13	
3	Benzaldehyde	956	960	0.30	
4	β -Pinene	972	1008	0.08	
5	α -Phellandrene	1002	1002	0.11	
6	α -Terpinene	1012	1017	0.16	
7	ρ -Cymene	1020	1024	1.23	
8	β -Phellandrene	1026	1029	1.67	
9	Salicylaldehyde	1028	1044	0.44	
10	Linalool	1101	1098	4.72	
11	α -Campholenal	1122	1126	0.19	
12	Camphor	1147	1141	7.96	
13	(Z)-Non-3-en-1-ol	1157	1152	0.42	
14	Borneol	1169	1169	0.79	
15	cis-Linalool oxide	1178	1174	1.66	
16	ρ -Cymen-8-ol	1182	1179	0.16	
17	Cryptone	1185	1183	0.14	
18	α -Terpineol	1194	1188	3.15	
19	γ -terpineol	1200	1199	0.18	
20	Hydrocinnamyl alcohol	1214	1227	0.53	
21	Nerol	1223	1229	0.13	
22	o-Anisaldehyde	1248	1239	0.15	
23	(E)-Cinnamaldehyde	1270	1267	33.31	
24	(E)-Cinnamyl alcohol	1300	1304	0.11	
25	Eugenol	1358	1359	11.37	

26	Hydrocinnamyl acetate	1369	1368	1.35	
27	Methyl eugenol	1395	1403	0.27	
28	β -Caryophyllene	1413	1417	3.58	
29	Ethyl cinnamate	1430	1422	0.10	
30	(<i>E</i>)-Cinnamyl acetate	1438	1443	0.16	
31	(<i>E</i>)-Cinnamic acid	1446	1454	0.79	
32	(<i>E</i>)-Methyl isoeugenol	1508	1492	0.20	
33	α -Muurolene	1510	1500	0.11	
34	2-methoxycinnamaldehyde	1522	1505	0.56	
35	α -Calacorene	1539	1545	0.13	
36	cis-3-Hexenyl benzoate	1566	1565	0.2	
37	Caryophyllene oxide	1573	1583	2.09	
38	Spathulenol	1583	1600	0.39	
39	Thujopsan-2- β -ol	1588	1589	0.17	
40	Globulol	1591	1590	0.12	
41	Viridiflorol	1598	1592	0.35	
42	Sesquithuriferol	1605	1604	0.74	
43	(<i>Z</i>)-Asarone	1617	1616	0.08	
44	α -Muurolol	1624	1646	0.22	
45	1-epi-cubenol	1628	1627	0.45	
46	α -Cadinol	1631	1644	0.10	
47	Agarospinol	1648	1648	0.87	
48	Himachalol	1653	1652	0.18	
49	7-epi- α -Eudesmol	1663	1662	0.75	

50	β -Eudesma-4(15), 7-dien-1-ol	1688	1688	0.13	
51	Benzyl benzoate	1765	1759	11.22	
52	Eudesm-7(11)-en-4-ol, acetate	1840	1840	0.16	
53	<i>trans</i> -Farnesyl acetate	1855	1846	0.13	
54	Phytol	1943	1942	0.09	
55	3(<i>Z</i>)-Cembrene A	1948	1947	0.10	
56	Hexadecanoic acid	1970	1960	0.34	
57	Benzyl cinnamate	2076	2092	0.09	
	Monoterpene hydrocarbons			3.63	
	Oxygenated monoterpenes			19.07	
	Sesquiterpene hydrocarbons			3.58	
	Oxygenated sesquiterpenes			7.09	
	Benzenoids			14.34	
	Phenylpropanoids			46.88	
	Others			0.76	
	Oxygenated diterpenes			0.19	
	Total identified			95.54	

3.4. Protein-protein interaction analysis of intersecting targets

One hundred twenty-four common intersecting targets were imported into the STRING database by setting the confidence level score as high (0.7) and removing the disconnected nodes. After de-weighting, the targets were imported into Cytoscape 3.9.1 software, and PPI network diagram was obtained with 124 nodes and 1522 edges (Fig. 3C). The topological screening of protein-protein interaction analysis of the network was done using Cytohubba plugin on the basis of degree centrality. The top 6 proteins were TNF, IL6, TLR4, STAT3, IL8 and NFkB (Fig. 3D).

3.5. GO enrichment and KEGG pathway analysis

Gene ontology (GO) analysis of 124 intersecting targets was carried out to understand the core targets involved in cellular component (CC), molecular function (MF), and biological process (BP). A total of 127 GO terms were considerably enriched, including 95 in BP, 16 in CC and 16 in MF, respectively. The top 10 terms of BP, CC, and MF were obtained at a threshold cutoff of $p < 0.05$ and $FDR < 0.01$, respectively (Fig. 4A). The results showed that all 124 intersecting targets were associated with biological processes (BP) such as inflammatory response, positive regulation of transcription from RNA polymerase II promoter, signal transduction, positive regulation of gene expression etc. In terms of molecular function, the targets were associated in protein binding, zinc ion binding, enzyme binding, ATP binding etc. The core genes enriched with cellular component (CC) were mainly related to plasma membrane, cytoplasm, cytosol, integral component of plasma membrane etc. In KEGG enrichment analysis, we obtained 193 signalling pathways at a threshold value of $p < 0.05$ and $FDR < 0.01$ (Fig. 4B). The dot plot diagram was used to represent the top 20 pathways linked to inflammation based on their $-\log P$ value. The most significant KEGG pathways related to inflammation were TNF signalling pathway, Toll-like receptor pathway and IL-17 signalling pathway. To further analyse the mechanism by which key targets are associated with the anti-inflammatory effect of CZEO, targets were uploaded in KEGG mapper for significant pathway analysis. The predictive targets of most representative inflammatory signalling pathway namely Toll-like receptor pathway was shown in Fig. 5, which demonstrated the involvement of 19 genes through PI3K-Akt signalling pathway, NF-kappa B signalling pathway, MAPK signalling pathway and JAK-STAT signalling pathway.

3.6. Molecular docking and molecular dynamics simulation

Molecular docking was carried out to measure the binding affinity of active constituents of CZEO and the hub target genes. Seven active constituents (hydrocinnamyl acetate, benzyl benzoate, ethyl cinnamate, benzyl cinnamate, cinnamic acid, α -muurolene and hexadecanoic) acid and six target proteins (TNF, IL6, TLR4, STAT3, IL8, and NFkB) were selected from network screening having high degree scores. The Pyrx software was employed for molecular docking. A higher negative docking score indicates a stronger binding

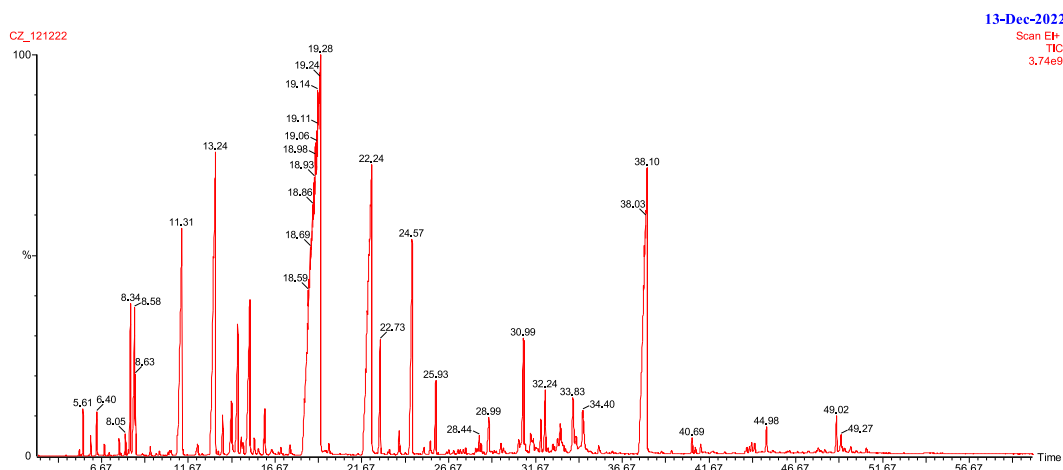


Fig. 2. Total ion chromatogram of *Cinnamomum zeylanicum* bark essential oil.

affinity between protein and ligand. The molecular docking results were presented as heat map, as depicted in Fig. 6A.

The binding affinities of target proteins with their active constituents and co-crystallized ligands/inhibitors are demonstrated in Table 5. It can be seen from Fig. 6A that benzyl benzoate with IL8 showed highest binding affinity of free binding energy -6.4 kcal/mol. This interaction was attributed to van der Waals forces with SER42, LEU47, TYR11 as well as hydrophobic interactions with ARG45, ASP43, PHE19, LEU41 and PHE15 residues of IL8 (Fig. 6B). Previously reparixinx-IL8 complex also displayed pi-pi stacking with PHE19 and alkyl interaction with LEU41 in agreement with the current study [26]. Additionally, we also discovered that benzyl cinnamate also exhibited good binding affinity towards STAT3 (-6.1 kcal/mol) by forming van der Waals interactions at ASP371, ASP369, VAL490, LEU436, HIS437, SER381, ARG382 and hydrophobic interactions at LYS383 residues of STAT3. Resveratrol interacted with STAT3 at the binding pocket by forming bonds with ASP369, LEU436, HIS437, SER381 amino acid residues in agreement with our study [27]. Similarly, α -muurolene interacted with STAT3 by forming van der Waals forces at LYS290, SER2922, TYR293, LEU207, PHE172, ASP173 and hydrophobic interactions at VAL291, TYR176, LYS177 residues of STAT3 having free binding energy of -6.1 kcal/mol.

Although molecular docking is a rapid and effective method for determining ligand-protein binding within a protein's active site, it overlooks the conformational stability that occurs during the interaction between the protein and ligand. In order to address this limitation, molecular dynamics (MD) simulation was employed for the docked complex as it will offer a more precise assessment of the conformational changes of stability and compatibility of protein-ligand complexes. The root mean square deviation (RMSD), the root mean square fluctuation (RMSF), and protein-ligand interactions were generated with the production of 100 ns MD simulations for the top ranked docked complex compared to the apo protein. The protein-ligand RMSD plots for the IL8-Benzyl benzoate complex showed that RMSD was greater than 3 \AA for the first few nanoseconds, increased to 4 \AA after a while, and then decreased to 3 \AA , where it stabilized (Fig. 7A). The fluctuation analysis, quantified as root-mean-square fluctuation (RMSF), revealed maximum fluctuation of $\sim 4 \text{ \AA}$ due to the inherent flexibility of N and C terminal loop residues. Active site residue involved in the interactions showed the least RMSF fluctuation ($\sim 1.5 \text{ \AA}$) throughout the simulation (Fig. 7B). The hydrogen-bond, hydrophobic contact, and ionic interaction are shown in interaction fraction in the Y-axis and the residues that aid in interaction are displayed in X-axis. While minor fluctuations in the Benzyl benzoate-IL8 interaction were noted during the simulation (Fig. 7C), crucial bonds established in the initial ligand-docked compounds remained consistent throughout. Through protein-ligand contact analysis, it was found that the residues Tyr11, Phe15, Phe19, Leu41, and Leu47 were responsible for hydrophobic contacts with benzyl benzoate, among which Tyr11, Phe15, Phe19 were the most accountable ones at 0.25 ns, 0.25 ns and 0.23 ns fractions of the interaction time, respectively. Arg45 was responsible for the highest water bridging at ns, while, on the other hand, Tyr11, Ser42, Asp43, and Arg45 were responsible for H-bonding contacts. The IL8-Benzyl benzoate exhibited stable dynamics as revealed by parameters RMSD, RMSF and intermolecular interactions.

3.7. CZEO did not affect the cell viability and morphology of RAW 264.7 cells

The cytotoxicity of CZEO on RAW 264.7 cells was measured using MTT assay. The result revealed that CZEO did not exhibit any cytotoxicity even at a dose of $100 \mu\text{g/ml}$ as more than 85 % of RAW 264.7 cells were viable (Fig. 8A). Therefore CZEO concentrations below $100 \mu\text{g/ml}$ were selected for subsequent assays. As observed in the untreated cells, the cell morphology generally showed a round and regular form (Fig. 8B). The treatment of RAW 264.7 cells with CZEO up to a concentration of $100 \mu\text{g/ml}$ did not exhibit much cell spreading and pseudopodia formation, indicating that most of the cells were viable. The results proposed that CZEO did not affect the viability and morphology of RAW 264.7 cells.

Table 3Drug likeness properties of the 52 screened compounds in *Cinnamomum zeylanicum* essential oil.

S. No.	Compound	Lipinski's rule				Abbott bioavailability Score (>0.5)	Lipinski Violation	Drug likeness
		MW (≤ 500) (g/mol)	MLOGP (<4.15)	HBA (<10)	HBD (<5)			
1	α -Thujene	136.23	4.29	0	0	0.55	1	Pass
2	α -Fenchene	136.23	4.29	0	0	0.55	1	Pass
3	Benzaldehyde	106.12	1.45	1	0	0.55	0	Pass
4	β -Pinene	136.23	4.29	0	0	0.55	1	Pass
5	α -Phellandrene	136.23	3.27	0	0	0.55	0	Pass
6	α -Terpinene	136.23	3.27	0	0	0.55	0	Pass
7	ρ -Cymene	134.22	4.47	0	0	0.55	1	Pass
8	β -Phellandrene	136.23	3.27	0	0	0.55	0	Pass
9	Salicylaldehyde	122.12	0.79	2	1	0.55	0	Pass
10	Linalool	154.25	2.59	1	1	0.55	0	Pass
11	α -Campholenal	152.23	2.2	1	0	0.55	0	Pass
12	Camphor	152.23	2.3	1	0	0.55	0	Pass
13	(Z)-Non-3-en-1-ol	142.24	2.39	1	1	0.55	0	Pass
14	Borneol	154.25	2.45	1	1	0.55	0	Pass
15	cis-Linalool oxide	170.25	1.38	2	1	0.55	0	Pass
16	ρ -Cymen-8-ol	150.22	2.49	1	1	0.55	0	Pass
17	Cryptone	138.21	1.89	1	0	0.55	0	Pass
18	γ -Terpineol	154.25	2.3	1	1	0.55	0	Pass
19	Hydrocinnamyl alcohol	136.19	2.19	1	1	0.55	0	Pass
20	Nerol	154.25	2.59	1	1	0.55	0	Pass
21	<i>o</i> -Anisaldehyde	136.15	1.12	2	0	0.55	0	Pass
22	(<i>E</i>)-Cinnamaldehyde	132.16	2.01	1	0	0.55	0	Pass
23	(<i>E</i>)-cinnamyl alcohol	134.18	2.1	1	1	0.55	0	Pass
24	Eugenol	164.2	2.01	2	1	0.55	0	Pass
25	Hydrocinnamyl acetate	178.23	2.58	2	0	0.55	0	Pass
26	Methyl eugenol	178.23	2.3	2	0	0.55	0	Pass
27	β -Caryophyllene	204.35	4.63	0	0	0.55	1	Pass
28	Ethyl Cinnamate	176.21	2.49	2	0	0.55	0	Pass
29	(<i>E</i>)-Cinnamyl acetate	176.21	2.49	2	0	0.55	0	Pass
30	(<i>E</i>)-Cinnamic acid	148.16	1.9	2	1	0.85	0	Pass
31	(<i>E</i>)-Methyl isoeugenol	178.23	2.3	2	0	0.55	0	Pass
32	α -Muuroleone	204.35	4.63	0	0	0.55	1	Pass
33	2-Methoxy-cinnamaldehyde	162.19	1.66	2	0	0.55	0	Pass
34	α -Calacorene	200.32	5.36	0	0	0.55	1	Pass
35	<i>cis</i> -3-Hexenyl benzoate	204.26	3.31	2	0	0.55	0	Pass
36	Caryophyllene oxide	220.35	3.67	1	0	0.55	0	Pass
37	Spathulenol	220.35	3.67	1	1	0.55	0	Pass
38	Globulol	222.37	3.81	1	1	0.55	0	Pass
39	Viridiflorol	222.37	3.81	1	1	0.55	0	Pass
40	Sesquithuriferol	222.37	3.81	1	1	0.55	0	Pass
41	(Z)-Asarone	208.25	1.97	3	0	0.55	0	Pass
42	α -Muurolol	222.37	3.67	1	1	0.55	0	Pass
43	1- <i>epi</i> -cubenol	222.37	3.67	1	1	0.55	0	Pass
44	α -Cadinol	222.37	3.67	1	1	0.55	0	Pass
45	Agarospirol	222.37	3.67	1	1	0.55	0	Pass
46	Himachalol	222.37	3.67	1	1	0.55	0	Pass
47	7- <i>epi</i> - α -Eudesmol	222.37	3.67	1	1	0.55	0	Pass
48	Benzyl benzoate	212.24	3.41	2	0	0.55	0	Pass
49	<i>trans</i> -Farnesyl acetate	264.4	4.14	0	9	0.55	1	Pass
50	Phytol	296.53	5.25	1	1	0.55	1	Pass
51	Hexadecanoic acid	256.42	4.19	2	1	0.85	1	Pass
52	Benzyl cinnamate	238.28	3.57	2	0	0.55	0	Pass

HBA: Hydrogen bond acceptor, HBD: Hydrogen bond donor, MLOGP: Moriguchi octanol-water partition coefficient.

3.8. CZEO treatment decreased the LPS-induced increase in nitric oxide (NO) and prostaglandin- E_2 (PGE $_2$) levels in RAW 264.7 cells

The inhibitory effect of CZEO on nitrite production in LPS-activated RAW 264.7 cells was evaluated using the Griess reagent. The result displayed a dose-dependent decrease in nitric oxide production in RAW 264.7 cells on treatment with varying concentrations of CZEO (Fig. 9A). LPS (1 μ g/ml) stimulation elevated the level of NO significantly ($^{#}p < 0.05$) in RAW 264.7 cells compared to the untreated group. However, exposure to different concentrations of CZEO significantly decreased nitric oxide levels in a concentration-dependent manner.

To explore the role of CZEO on PGE $_2$ production levels, RAW 264.7 cells were treated with LPS (1 μ g/ml) for 2 h followed by treatment with CZEO for 24 h. Stimulation of RAW 264.7 cells with LPS (1 μ g/ml) led to an inflammatory condition which led to a

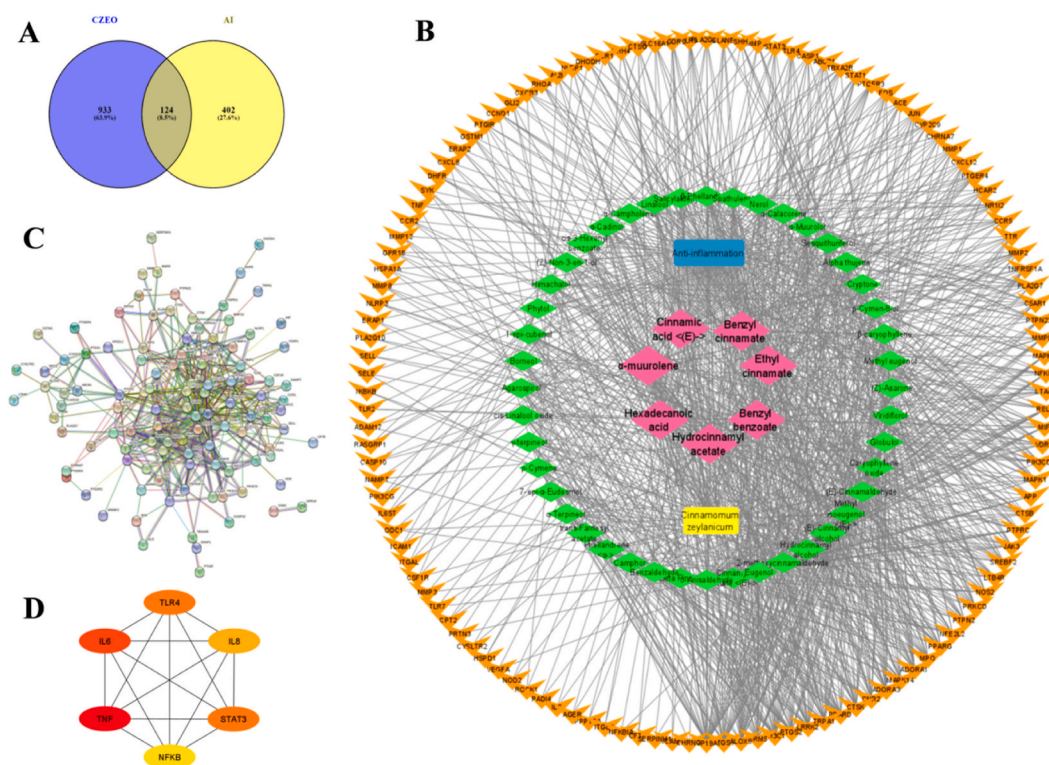


Fig. 3. Compound target network and protein protein interaction (PPI) analysis. (A) Venn diagram representing 124 targets of CZE0 against inflammation. (B) Compound-target network constructed using Cytoscape version 3.9.1. Pink diamonds represent hub compound with highest degree values and orange arrows represent targets. (C) Protein protein interaction network of 124 common targets resulted from STRING database containing 124 nodes and 1522 edges. (D) Topological screening of PPI network representing 6 hub genes.

significant increase ($^{\#}p < 0.05$) in the level of PGE₂ production compared to the untreated group (Fig. 9B). This rise in PGE₂ levels was remarkably reduced after treating the cells with CZE0 at concentrations of 12.5 $\mu\text{g/ml}$ and 100 $\mu\text{g/ml}$ by 1.03-fold and 4.30-fold, respectively.

3.9. CZE0 treatment decreased the LPS-induced increase in pro-inflammatory cytokines levels in RAW 264.7 cells

RAW 264.7 cells express IL-6, IL-1 β and TNF- α in response to LPS stimulation. Therefore, it was determined if CZE0 had any influence on the expression of inflammatory cytokines in LPS-induced RAW 264.7 cells. The levels of IL-1 β , IL-6 and TNF- α significantly ($^{\#}p < 0.05$) increased from 27.31 to 417.98 pg/ml, 33.50–358.71 pg/ml and 780.93–2447.48 pg/ml, respectively after treatment of RAW 264.7 cells with LPS (1 $\mu\text{g/ml}$). Treatment of CZE0 at concentrations of 12.5 and 100 $\mu\text{g/ml}$ effectively inhibited the expression level of IL-1 β by 6.56 % (1.07-fold) and 81.21 % (5.3-fold), IL-6 by 23.38 % (1.3-fold) and 81.13 % (5.3-fold), TNF- α by 42.85 % (1.7-fold) and 81.54 % (5.4-fold), respectively (Fig. 10A–C).

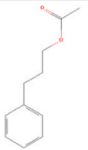
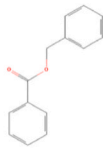
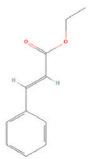
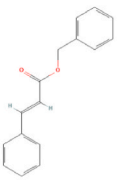
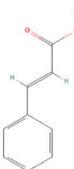
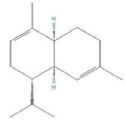
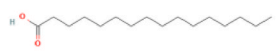
3.10. CZE0 treatment increased LPS-induced decrease in endogenous antioxidant levels in RAW 264.7 cells

The antioxidation system includes antioxidant enzymes, which are crucial in lowering ROS levels. Cells were stimulated with LPS, followed by exposure to different doses of CZE0. LPS stimulation reduced SOD, CAT, GPx and GSH levels in RAW 264.7 cells. In contrast to LPS-treated cells, however, treatment with CZE0 at doses of 12.5 and 100 $\mu\text{g/ml}$ dramatically increased the SOD level by 1.86 and 7.55 fold, respectively (Fig. 11A). The basal levels of GSH were increased by 1.5 and 3.32 fold (Fig. 11B), CAT by 4.2 and 12.8 fold (Fig. 11C), and GPx by 1.3 and 6 fold (Fig. 11D), respectively, when cells were treated with CZE0 at doses of 12.5 and 100 $\mu\text{g/ml}$.

3.11. CZE0 treatment decreased LPS-induced increase in ROS level in RAW 264.7 cells

The antioxidant activity conferred by CZE0 in LPS-treated RAW 264.7 cell is associated with a reduction in intracellular ROS generation, which was assessed using oxidation-sensitive probe 2',7'-dichlorodihydrofluorescein di-acetate (DCFH-DA) by flow cytometry (Fig. 12A). RAW 264.7 cells treated with LPS led to a significant ($^{\#}p < 0.05$) increase in the intracellular ROS level as compared to the untreated group, which was effectively attenuated by treating with CZE0 in a dose-dependent manner (Fig. 12B).

Table 4
Active constituents of *Cinnamomum zeylanicum* essential oil based on degree centrality.

Compound	Structure	Pubchem ID	Molecular formula	Molecular weight (g/mol)	Degree
Hydrocinnamyl acetate		31226	C ₁₁ H ₁₄ O ₂	178.23	50
Benzyl benzoate		2345	C ₁₄ H ₁₂ O ₂	212.24	50
Ethyl cinnamate		637758	C ₁₁ H ₁₂ O ₂	176.21	44
Benzyl cinnamate		5273469	C ₁₆ H ₁₄ O ₂	238.28	37
Cinnamic acid		444539	C ₉ H ₈ O ₂	148.16	32
α -Muurolene		12306047	C ₁₅ H ₂₄	204.35	31
Hexadecanoic acid		985	C ₁₆ H ₃₂ O ₂	256.42	31

3.12. CZEO treatment protected mitochondrial membrane potential from LPS induced depolarization in RAW 264.7 cells

To investigate the role of CZEO on LPS-mediated mitochondrial membrane damage, RAW 264.7 macrophages were treated with mitochondrial-membrane probe JC-1 dye and observed under microscope. Intact mitochondrial membrane potential caused the JC-1 to fluoresce green and damaged membrane potential caused the JC-1 to fluoresce red. This depletion in mitochondrial membrane potential was significantly restored when RAW 264.7 cells were treated with CZEO at concentrations of 12.5 and 100 μ g/ml, respectively (Fig. 13A–D).

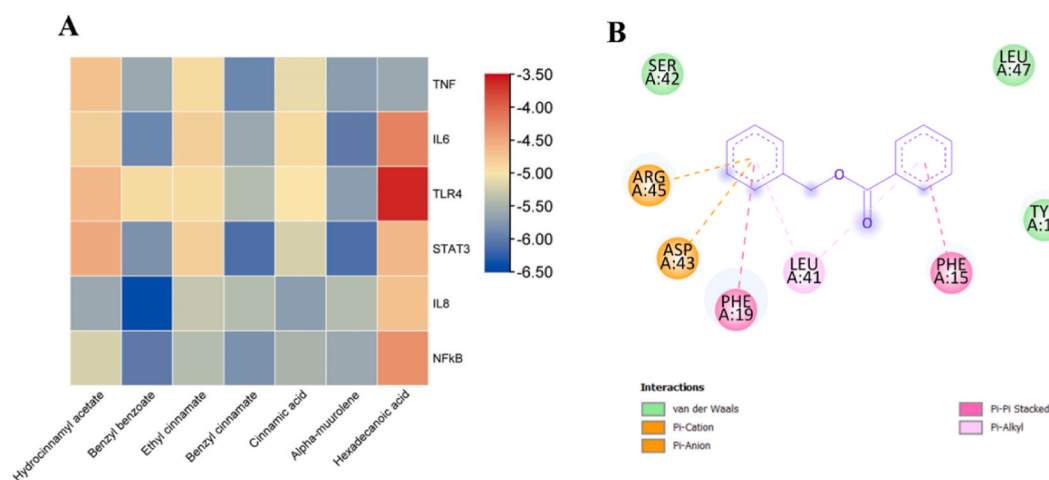


Fig. 6. Molecular docking analysis of core constituents of CZEO with hub targets. (A) Heat map showing binding affinities between hub targets with probable drug ligands. (B) Molecular docking simulation showing interaction between protein and ligand of highest binding affinity i.e. IL8 with benzyl benzoate.

3.14. CZEO exert anti-inflammatory effect by modulating toll-like receptor pathway in RAW 264.7 cells

It was observed from network pharmacology analysis that CZEO exert anti-inflammatory effect by modulating Toll-like receptor pathway. Therefore we investigated the effect of CZEO on down-stream target genes involved in Toll-like receptor pathway by assessing their mRNA expression levels using RT-qPCR. RAW 264.7 cells were treated with LPS (1 $\mu\text{g}/\text{ml}$) followed by treatment with CZEO (12.5 and 100 $\mu\text{g}/\text{ml}$) and incubated for 24 h. In LPS stimulated RAW 264.7 cells, CZEO treatment reduce the mRNA expression level of TLR4, IL8, IL6, NFKB and TNF in a dose dependent manner compared to that of LPS treated group (Fig. 15A–E)

4. Discussion

Inflammation has been linked to the development and progression of various chronic diseases [28,29]. The adverse reactions caused by long-term usage of non-steroidal anti-inflammatory drugs (NSAIDs) and steroidal anti-inflammatory drugs (SAIDs) are gradually increasing and garnering public attention. In recent years, there has been a growing evidence that herbal medicines significantly reduce inflammation [13]. The bark of *Cinnamomum zeylanicum* is used in herbal medicines for treating inflammation and pain [30]. Previous research has shown that *Cinnamomum zeylanicum* essential oil possesses anti-inflammatory properties [19,31], however, its molecular mechanism remains unelucidated. Therefore, network pharmacology in combination with *in vitro* assays was applied to identify the effective constituents, molecular targets and to explore the potential mechanism of *Cinnamomum zeylanicum* essential oil in treating inflammation.

In this study, a total of 57 constituents were identified by GC-MS analysis, including phenylpropanoids, oxygenated monoterpenes, monoterpene hydrocarbons, benzenoids, sesquiterpene hydrocarbons, oxygenated sesquiterpenes, and diterpenoids. Numerous studies have revealed that phenylpropanoids, including cinnamaldehyde, cinnamic acid, and methyl eugenol, inhibit tissue inflammation and modulate signalling pathways involved in the inflammatory response [32–35]. Cinnamaldehyde has been reported to possess anti-inflammatory, anti-microbial, anti-diabetic properties [18]. E-Cinnamaldehyde and O-methoxy cinnamaldehyde has been shown to display potent anti-inflammatory activity by inhibiting the production of LPS + IFN- γ induced NO and TNF- α in RAW 264.7 and J774A.1 cells. Certain major constituents like coumarin and cinnamyl alcohol which were present in bark extracts of *Cinnamomum zeylanicum* were not detected in the essential oil [36]. This might be due to the fact that compounds present in essential oil are mostly volatile constituents, whereas that in extracts are usually non-volatile compounds. It is imperative to carry out pharmacokinetic parameter screening of herbal medicine to obtain active constituents [37]. After screening compounds for drug-likeness (Lipinski's rule) and bioavailability score (Abbott), 52 active compounds were retrieved. The compound target disease network was then constructed using Cytoscape software, which revealed hydrocinnamyl acetate (degree-50), benzyl benzoate (degree-50), ethyl cinnamate (degree-44), benzyl cinnamate (degree-37), cinnamic acid (degree-32), α -muurolene (degree-31), and hexadecanoic acid (degree-31) to exhibited higher degree values than other constituents. We found that the important component of *Cinnamomum zeylanicum* essential oil, such as benzyl benzoate plays a crucial role in alleviating skin inflammation in patients suffering from rosacea and demodicosis [38,39]. Anti-inflammatory property of ethyl cinnamate using albumin denaturation activity has also been studied [40]. Cinnamic acid has shown vasodilative property activity in human umbilical vein endothelial cells by modulating nitric oxide-cGMP-PKG pathway [41]. Benzyl cinnamate has been reported to possess a myriad of bioactivities, such as anti-inflammatory, anti-cancer, anti-ultraviolet radiation, and anti-fungal effects [42,43]. Hexadecanoic acid acts as an anti-inflammatory agent by inhibiting the activity of phospholipase A₂ [44].

The PPI network of gene targets for *Cinnamomum zeylanicum* essential oil in treating inflammation was established based on the

Table 5
Binding affinities of target proteins with active constituents and co-crystallized ligands/inhibitors.

Protein	Compounds	Binding affinity (kcal/mol)
TNF (PDB ID: 2AZ5)	Hydrocinnamyl acetate	-4.7
	Benzyl benzoate	-5.6
	Ethyl cinnamate	-4.9
	Benzyl cinnamate	-5.9
	Cinnamic acid	-5.1
	α -Muuroleone	-5.7
	Hexadecanoic acid	-5.6
IL6 (PDB ID: 1ALU)	3-phenyl-propenal	-4.7
	Hydrocinnamyl acetate	-4.8
	Benzyl benzoate	-5.9
	Ethyl cinnamate	-4.8
	Benzyl cinnamate	-5.6
	Cinnamic acid	-4.9
	α -Muuroleone	-6
TLR4 (PDB ID: 2Z63)	Hexadecanoic acid	-4.2
	ι (+)-TARTARIC ACID	-4.7
	Hydrocinnamyl acetate	-4.6
	Benzyl benzoate	-4.9
	Ethyl cinnamate	-4.9
	Benzyl cinnamate	-5.4
	Cinnamic acid	-5
STAT3 (PDB ID: 6NJS)	α -Muuroleone	-5.7
	Hexadecanoic acid	-3.6
	TLR4-IN-C34	-4.9
	Hydrocinnamyl acetate	-4.5
	Benzyl benzoate	-5.8
	Ethyl cinnamate	-4.8
	Benzyl cinnamate	-6.1
IL8 (PDB ID: 6N2U)	Cinnamic acid	-5.2
	α - muuroleone	-6.1
	Hexadecanoic acid	-4.6
	KQV	-9.3
	Hydrocinnamyl acetate	-5.6
	Benzyl benzoate	-6.4
	Ethyl cinnamate	-5.3
NFKB (PDB ID: 1NFI)	Benzyl cinnamate	-5.4
	Cinnamic acid	-5.7
	α -Muuroleone	-5.4
	Hexadecanoic acid	-4.7
	Reparixin	-5.6
	Hydrocinnamyl acetate	-5.2
	Benzyl benzoate	-6
	Ethyl cinnamate	-5.4
	Benzyl cinnamate	-5.8
	Cinnamic acid	-5.5
	α -Muuroleone	-5.6
	Hexadecanoic acid	-4.3
	JSH-23	-4.9

compound and inflammatory target network with 124 intersecting genes. Using the degree algorithm of the CytoHubba plug-in, 6 hub genes, namely TNF, IL6, TLR4, IL8, STAT3 and NFKB with the highest degree values were identified. The docking results of these targets also revealed that the compounds had a high binding affinity for them. TNF- α plays a critical role in accelerating wound healing and excessing inflammation by impairing leukocyte recruitment and NFKB activation [45]. Toll-like receptor 4 (TLR4) pathway is a promising strategy to target several pathologies, including arteriosclerosis, rheumatoid arthritis, neuroinflammation, trauma and haemorrhage [46]. IL6 inhibition has effectively prevented inflammation, as tested in various chronic inflammatory disease models such as colitis and arthritis [47]. A key player in the pathogenesis of lung inflammatory illness is the pro-inflammatory cytokine IL-8, which attracts neutrophils to the site of inflammation [48]. Signal transducer and activator of transcription (STAT3) plays a central role in the host's response to injury by maintaining homeostasis [49]. NF-kB is a pleiotropic transcription factor activated in response to foreign stimuli and is involved in immune response, inflammation, cellular proliferation, differentiation and survival [50,51]. The docking results of the identified targets also revealed that *Cinnamomum zeylanicum* essential oil compounds have a good binding affinity for these genes, further supporting their potential use as anti-inflammatory agents. Overall, these findings suggest that *Cinnamomum zeylanicum* essential oil may be a promising natural remedy for inflammatory diseases, potentially targeting multiple targets and pathways simultaneously.

The GO enrichment analysis proposed that the intersecting genes were involved in several biological processes, such as inflammatory response, positive regulation of transcription from RNA polymerase II promoter, signal transduction, positive regulation of

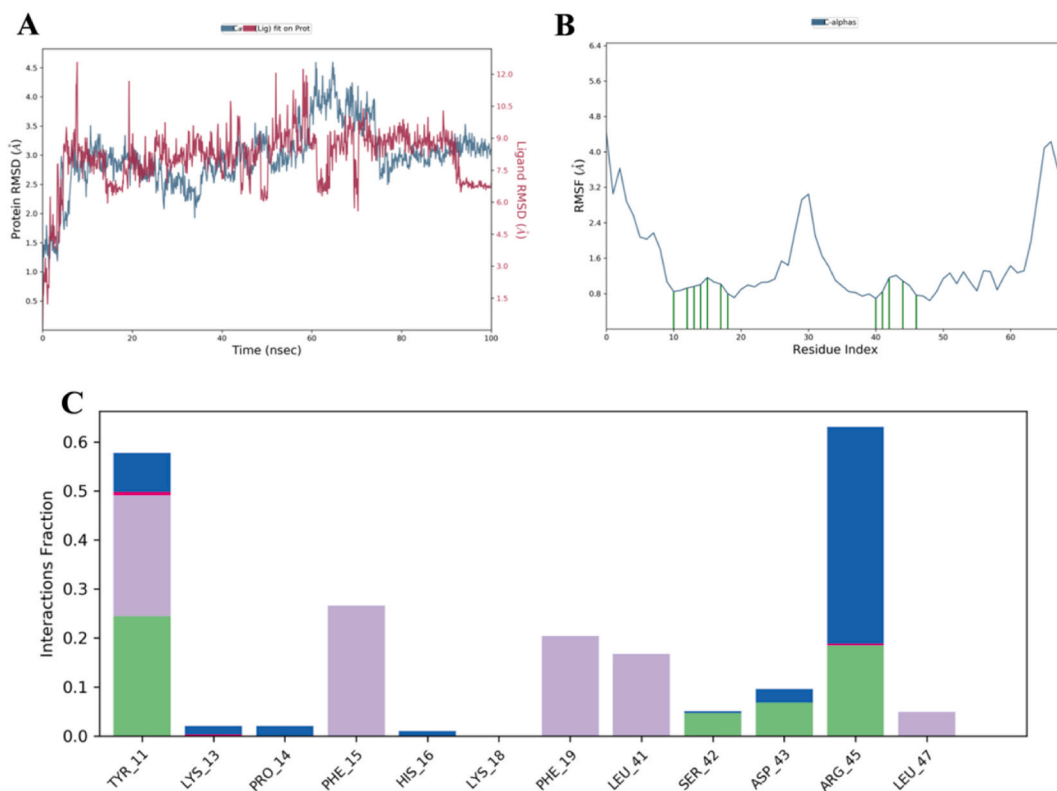


Fig. 7. MD simulation of IL8 and benzyl benzoate complex (A) Protein-ligand RMSD of IL8-benzyl benzoate complex during 100 ns MD simulation (B) C-alpha root mean square fluctuation of IL8 during 100 ns MD simulation (C) Histogram of protein-ligand contacts resulted from MD simulation of IL8 with benzyl benzoate complex.

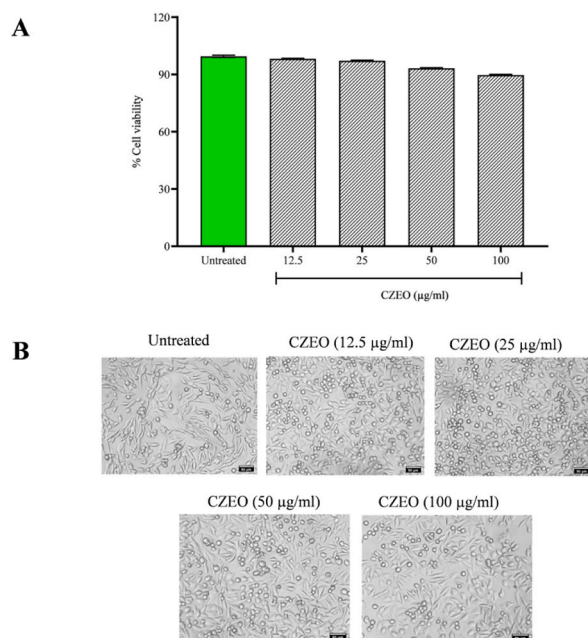


Fig. 8. Protective role of *Cinnamomum zeylanicum* essential oil (CZEO) on cell viability and morphological alteration in RAW 264.7 cells. (A) Cytotoxicity effect of CZEO on RAW 264.7 cells as measured by MTT assay (B) Cells were treated with various concentration of CZEO (12.5–100 µg/ml) for 24 h and the morphology was observed under microscope (scale bar 50 µm). Data are expressed as mean \pm SD of three independent experiments.

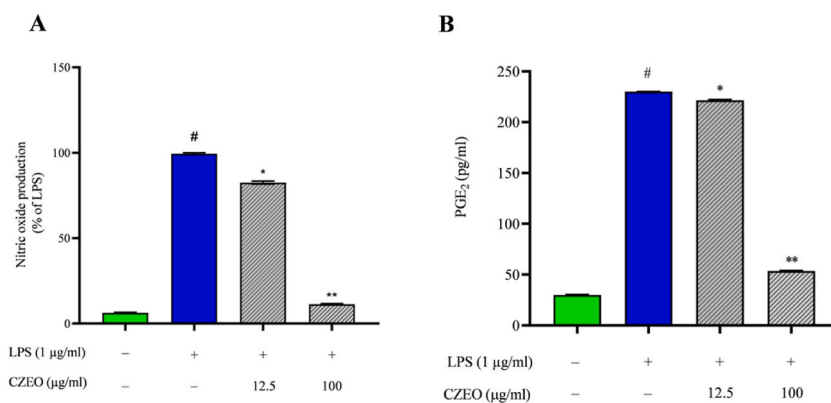


Fig. 9. Effect of CZEO on LPS-induced nitric oxide (NO) and prostaglandin-E₂ (PGE₂) production in RAW 264.7 cells. Cells were treated with LPS (1 µg/ml) for 2 h followed by treatment with CZEO (12.5 and 100 µg/ml) for 24 h. Measurement of (A) NO and (B) PGE₂ levels. Data are expressed as mean ± SD (n = 3). Statistical significance was measured by using one way analysis of variance followed by Tukey test. #*p* < 0.05 between untreated and LPS-treated group; **p* < 0.05, ***p* < 0.01 between LPS and CZEO treated group.

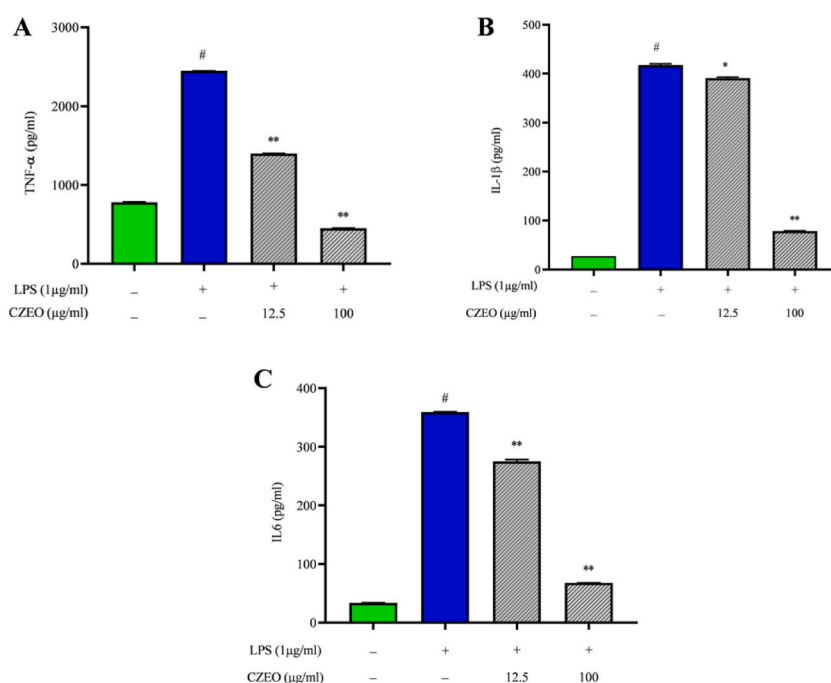


Fig. 10. Effect of CZEO on LPS-induced pro-inflammatory cytokine expression in RAW 264.7 cells. Cells were treated with LPS (1 µg/ml) for 2 h followed by treatment with CZEO (12.5 and 100 µg/ml) for 24 h. Cell-free supernatants were collected to estimate the level of (A) TNF-α, (B) IL-1β and (C) IL6 cytokines. Data are expressed as mean ± SD (n = 3). Statistical significance was measured by using one way analysis of variance followed by Tukey test. #*p* < 0.05 between untreated and LPS-treated group; **p* < 0.05 and ***p* < 0.01 between LPS and CZEO treated group.

gene expression etc, thus suggesting that the anti-inflammatory activity of CZEO is due to modulation of these processes. Immediate mediators of the inflammatory response have a specific mechanism that involves RNA polymerase II stalling to facilitate their gene activation [52]. Many chronic inflammatory diseases are associated with deregulated intracellular signal transduction pathways [53].

KEGG enrichment analysis indicated that TNF signalling pathway, Toll-like receptor signalling pathway and IL-17 signalling pathway were the critical signalling pathways involved in inflammation. In the Toll-like receptor signalling pathway, LPS enters the host body by interacting with TLR4 and triggers the activation of numerous inflammatory mediators. Therefore, inhibition of TLR signalling pathways is an excellent strategy to control inflammation. Previous studies revealed the anti-inflammatory activity of several essential oils by down-regulating TLR4/NFκB pathway in LPS-induced RAW 264.7 cells [54,55].

Our findings reported that CZEO contains seven core compounds (benzyl benzoate, hydrocinnamyl acetate, ethyl cinnamate, benzyl cinnamate, cinnamic acid, α-murolene, and hexadecanoic acid) that can be linked to six potential target genes (TNF, IL6,

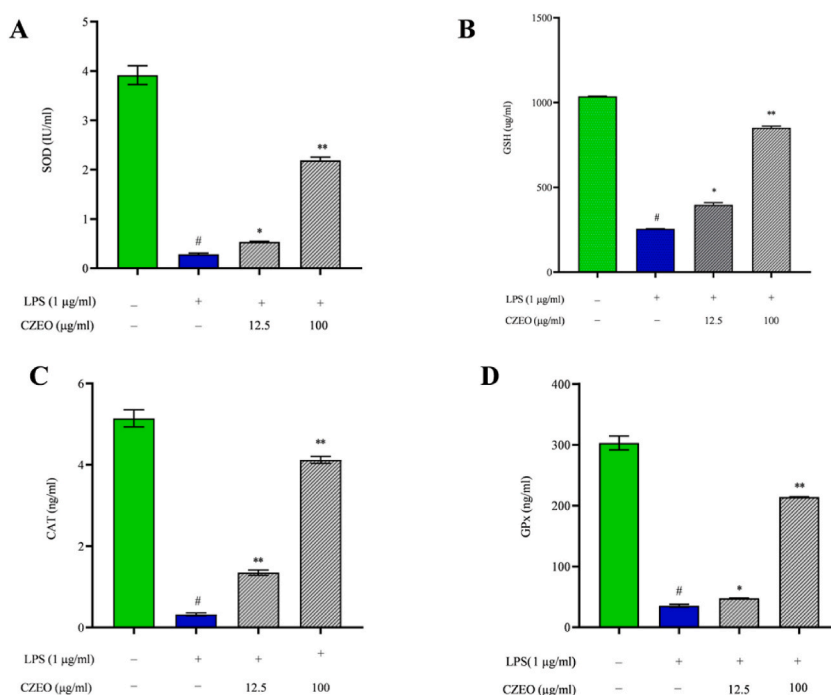


Fig. 11. Effect of CZEО on the endogenous anti-oxidant enzymes in LPS stimulated RAW 264.7 cells. Cells were treated with LPS (1 µg/ml) for 2 h followed by treatment with CZEО (12.5 and 100 µg/ml) for 24 h. Antioxidant enzymes including (A) SOD, (B) CAT, (C) GSH, and (D) GPx levels were assessed from cell free supernatant. Data are expressed as mean \pm SD ($n = 3$). Statistical significance was measured by using one way analysis of variance followed by Tukey test. # $p < 0.05$ between untreated and LPS-treated group; * $p < 0.05$ and ** $p < 0.01$ between LPS and CZEО treated group.

TLR4, IL8, STAT3 and NFKB) related to inflammation. These six potential target proteins associated with seven active compounds selected by network pharmacology analysis were further analyzed by molecular docking simulation. This determined the binding pose of the active compounds when bound to the target protein, and suggested that the active compounds might have high binding affinity for proteins encoded by inflammation-related genes. The molecular docking score indicated that the significant node (benzyl benzoate), which had a high degree obtained from network analysis, had the strongest affinity with probable target genes. Additionally, according to prior studies, benzyl benzoate substantially reduces inflammation of the skin [37]. This finding suggests that one or more compounds may interact with many target proteins instead of just one molecule and one target protein. Thus, we validated the premise that the anti-inflammatory efficacy of CZEО results from the interaction of many active compounds and multiple target genes and/or proteins.

Meanwhile, *in vitro* assays were performed on LPS-induced RAW 264.7 cells to support the findings revealed by network pharmacology and to decipher the anti-inflammatory action of CZEО. CZEО did not exhibit cytotoxicity on RAW 264.7 cells, even at a dose of 100 µg/ml, as more than 85 % of the cells remained viable. Therefore, concentrations below 100 µg/ml were chosen for subsequent assays. Additionally, the NO inhibitory activity of CZEО was tested using the Griess assay. Nitric oxide is a pro-inflammatory mediator and is a critical element in the pathophysiology of inflammation [56]. It was observed that CZEО revealed anti-inflammatory properties by inhibiting nitric oxide (NO) levels. PGE₂ is another key inflammatory mediator synthesized via the arachidonic acid metabolism pathway that plays a critical role in the vasodilation of infiltrating leukocytes and the recruitment of macrophages at the inflammation site [57]. Numerous studies suggest that uncontrolled generation of pro-inflammatory cytokines like TNF, IL-1 β , and TNF- α are associated with inflammatory injuries and pathogenesis of inflammation [58,59]. Therefore, in this study, the levels of pro-inflammatory cytokines were evaluated after treating LPS RAW 264.7 cells with CZEО. It was observed that CZEО significantly suppressed the expression levels of PGE₂, IL-6, IL-1 β , and TNF- α in RAW 264.7 macrophages compared to the LPS-treated group.

Another key inflammation factor is oxidative stress created by reactive oxygen species (ROS). ROS functions as a secondary messenger in various signalling pathways including apoptosis, inflammation, cell growth [7]. Oxidative stress is defined as a state of imbalanced oxidant/anti-oxidant ratio in the body leading to oxidative damage of cellular organelles [9,60]. Excessive ROS destroy mitochondrial membrane integrity and lead to the advancement of chronic inflammation [61,62]. Adverse effects exerted by ROS are neutralized by a natural antioxidant defence system. A delicate balance between oxidants and antioxidant maintains homeostasis [63]. Therefore, in this study, we assessed the level of intracellular ROS and measured the levels of antioxidant enzymes such as SOD, CAT, GPx and GSH in LPS-induced RAW 254.7 cells. It was observed that CZEО inhibited LPS-mediated ROS accumulation, restored mitochondrial membrane potential and increased the level of antioxidant enzymes in RAW 264.7 cells.

Intracellular ROS stimulate the secretion of cytokines by activating the NF- κ B transcription factor [64]. NF- κ B exists as a

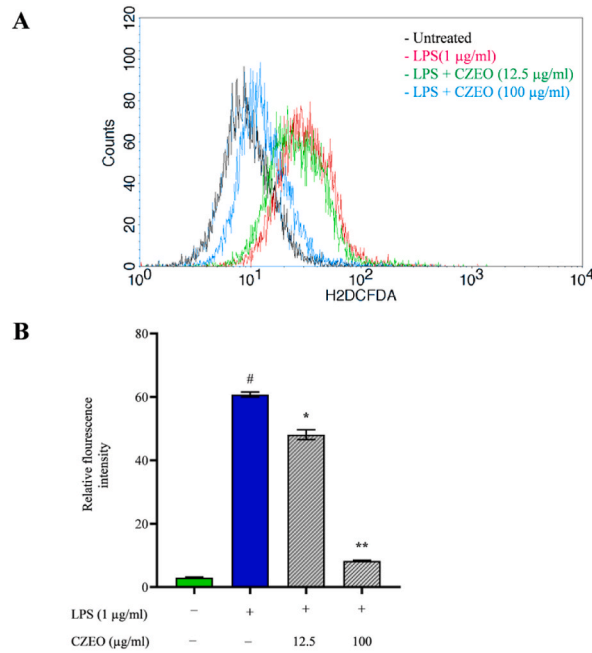


Fig. 12. Change in intracellular ROS levels in LPS stimulated RAW 264.7 cells after treatment with CZEO as measured by flow cytometry. Cells were treated with LPS (1 µg/ml) for 2 h followed by treatment with CZEO (12.5 and 100 µg/ml) for 24 h. After incubation cells were incubated with DCFH-DA for 30 min. (A) Fluorescence intensity plots of DCF dye in untreated cells (black color) and cells exposed to LPS (red color) and then treated with 12.5 µg/ml of CZEO (green color) and 100 µg/ml of CZEO (blue color). The probe DCFH-DA was incubated in cells for 30 min. (B) Quantitative analysis represented as relative fluorescence intensity of each treated group. Data are expressed as mean ± SD (n = 3). Statistical significance was measured by using one way analysis of variance followed by Tukey test. #*p* < 0.05 between untreated and LPS-treated group; **p* < 0.05 and ***p* < 0.01 between LPS and CZEO treated group.

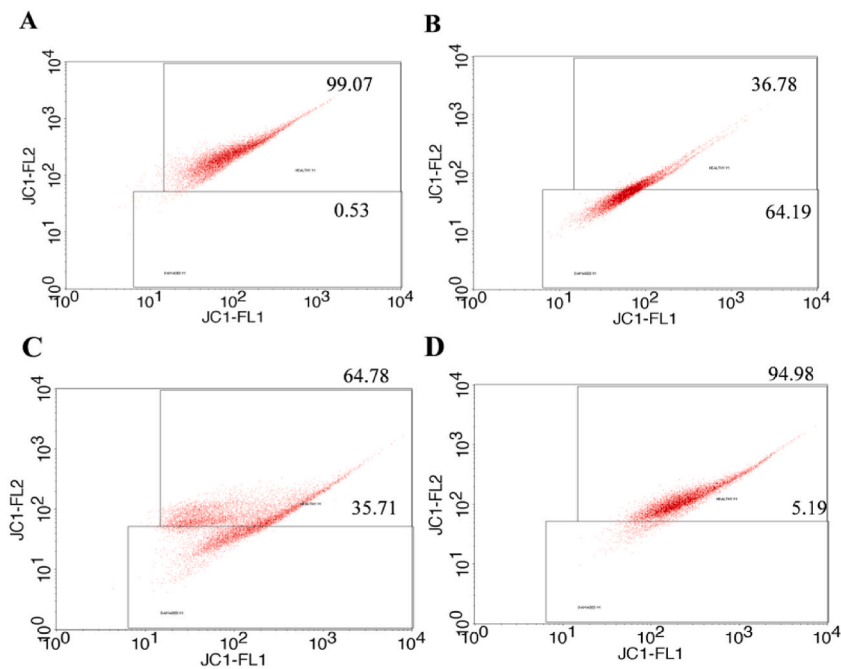


Fig. 13. Analysis of change in mitochondrial membrane potential in LPS stimulated RAW 264.7 cells after treatment with CZEO as measured by flow cytometry using JC-1 assay. Cells were treated with LPS (1 µg/ml) for 2 h followed by treatment with CZEO (12.5 and 100 µg/ml) for 24 h. After incubation cells were stained with JC-1 dye for 30 min. Data are presented as dot plot of JC-1 red fluorescence representing healthy mitochondria (Y-axis) against JC-1 green fluorescence representing damaged mitochondria (X-axis). (A) Untreated group (B) LPS treated group (C) CZEO treated group (12.5 µg/ml) (D) CZEO treated group (100 µg/ml).

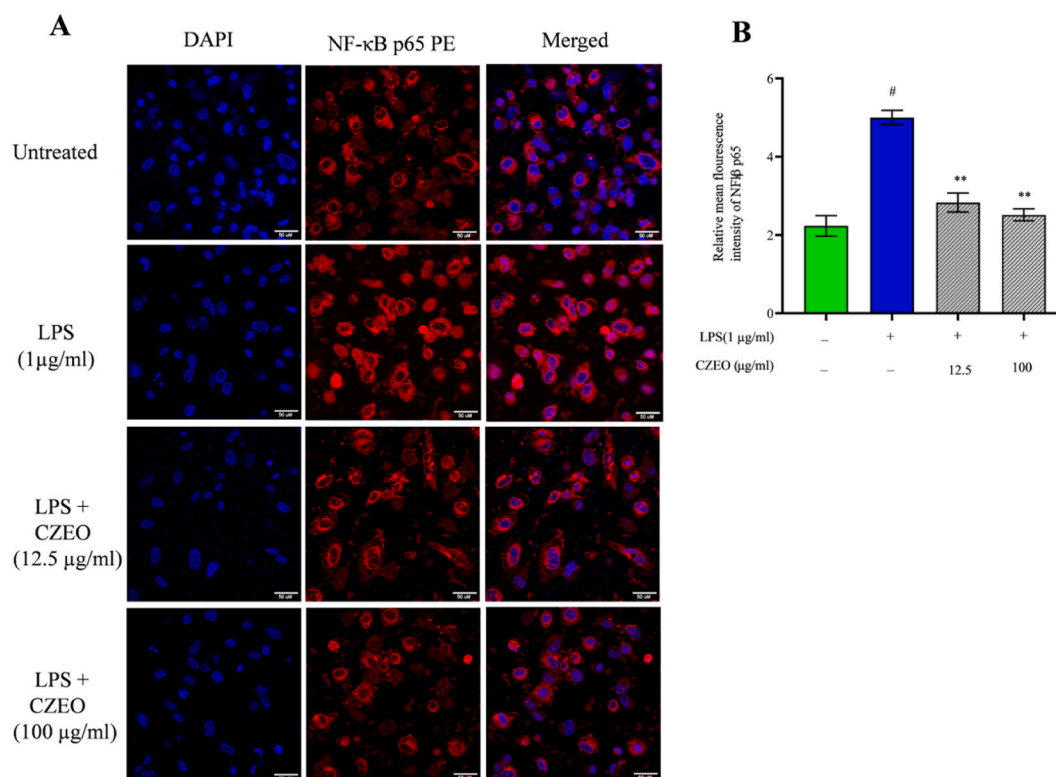


Fig. 14. Effect of CZEO on LPS induced nuclear translocation of NF-κB p65 in RAW 264.7 cells. Cells were treated with LPS (1 μg/ml) for 2 h followed by treatment with CZEO (12.5 and 100 μg/ml) for 24 h. (A) Representative confocal images of NF-κB p65 nuclear translocation in RAW 264.7 cells in different treated groups. RAW 264.7 cells are stained with DAPI (blue color) and immunolabelled for NFκB p65 (red color). Bar represents 50 μm (B) Quantitative analysis represented as relative mean fluorescence intensity of NF-κB p65 of each treated group. Data are expressed as mean ± SD (n = 3). Statistical significance was measured by using one way analysis of variance followed by Turkey test. [#]*p* < 0.01 between untreated and LPS treated group; ^{**}*p* < 0.01 between LPS and CZEO treated group.

heterodimeric complex of p50 and p65 subunits and LPS stimulation can induce the transcriptional activity of NF-κB p65 by promoting its nuclear translocation. NF-κB remains in inactive cytoplasmic form by binding with the inhibitory protein IκB. Upon LPS stimulation, p65 subunit is separated, and IκB undergoes phosphorylation and degradation, thereby translocating activated NF-κB p65 into the nucleus and resulting in the release of cytokines [65,66]. Therefore, in the current study, we assessed the effect of CZEO on NF-κB p65 nuclear translocation. The results revealed that CZEO effectively inhibited the nuclear translocation of NF-κB p65 in a dose-dependent manner. The current finding is in agreement with the result reported by another researcher, who also demonstrated another key *Cinnamomum* species i.e. *Cinnamomum subavenium* essential oil to exert an anti-inflammatory effect in carrageenan-induced paw edema mouse model by antagonizing the transcriptional activity of NF-κB [67].

Additionally, RT-qPCR analysis was carried out to understand the role of CZEO on the mRNA expression level of downstream target genes involved in Toll-like receptor pathway in RAW 264.7 cells. The results of RT-qPCR implied that CZEO treatment downregulated the mRNA expression of TLR4, IL8, IL6, TNF and NFκB that were upregulated after treating RAW 264.7 cells with LPS, thereby suggesting that CZEO could alleviate inflammation in RAW 264.7 cells mainly via Toll-like receptor signalling pathway.

5. Conclusions

In summary, a combination of network pharmacology and experimental assays was carried out to systematically validate the active constituents of CZEO and its multitarget and multi-pathway characteristics in the process of treating inflammation. The key targets predicted from network pharmacology were verified in the LPS-induced RAW 264.7 inflammation model. The present study showed that CZEO could alleviate inflammation in RAW 264.7 cells mainly via toll like receptor signalling pathway. Hydrocinnamyl acetate, benzyl benzoate, ethyl cinnamate, benzyl cinnamate, cinnamic acid, α-murolene and hexadecanoic acid may be the key active constituents behind the anti-inflammatory effect of CZEO. However, we still have a limited understanding of how these active compounds induce a protective effect on LPS induced inflammation. Secondly, because the current study was based on network pharmacology and *in vitro* assays, further experiments on animal models are still needed to validate the anti-inflammatory activity of CZEO. Thirdly, some compounds of CZEO have been detected by GC-MS and this may produce bias in our study. Overall, the obtained results suggested that CZEO might be used as a promising therapeutic agent for treating inflammation-related disorders.

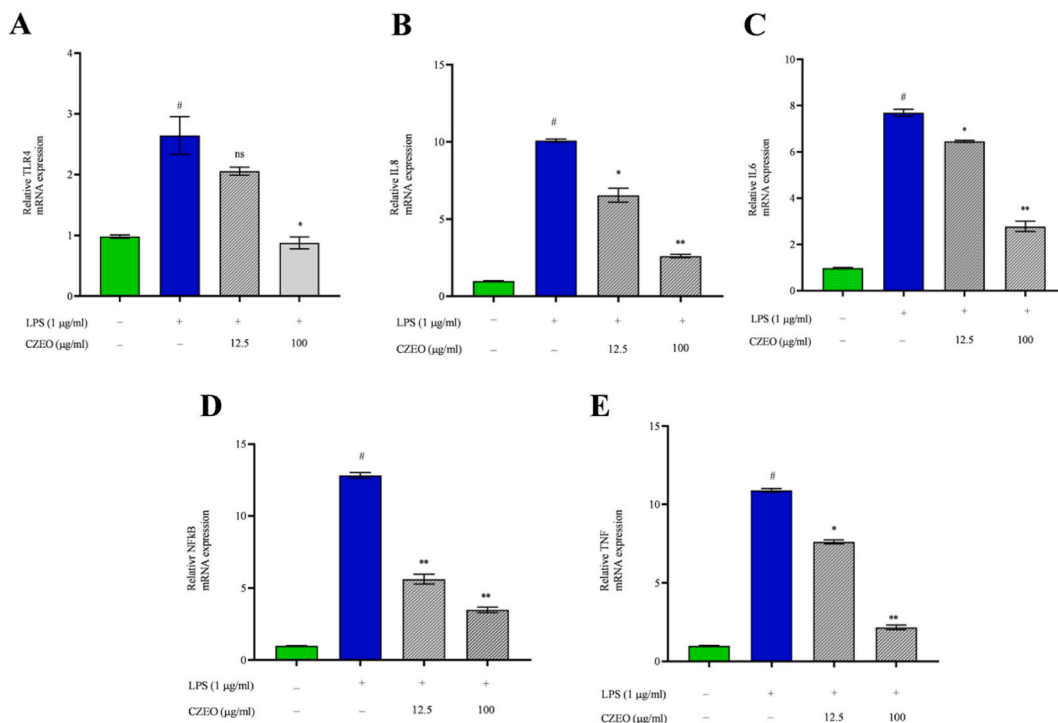


Fig. 15. Effect of CZE0 on expression level of downstream genes involved in Toll like receptor pathway. mRNA expression of (A) TLR4 (B) IL8 (C) IL6 (D) NFkB and (E) TNF genes identified by RT-qPCR. Cells were treated with LPS (1 µg/ml) for 2 h followed by treatment with CZE0 (12.5 and 100 µg/ml) for 24 h. Data are expressed as mean ± SD (n = 3). Statistical significance was measured by using one way analysis of variance followed by Tukey test. #*p* < 0.05 between untreated and LPS treated group; ^{ns}*p* > 0.05, **p* < 0.05 and ***p* < 0.01 between LPS and CZE0 treated group.

Funding

This work received no funds or any extramural research grants.

Data availability statement

Data will be made available on request.

Additional information

No additional information is available for this paper.

CRedit authorship contribution statement

Debjani Mohanty: Data curation, Investigation, Writing - original draft. **Suheetmita Padhee:** Data curation. **Chiranjibi Sahoo:** Data curation. **Sudipta Jena:** Data curation. **Ambika Sahoo:** Data curation. **Pratap Chandra Panda:** Data curation. **Sanghamitra Nayak:** Data curation. **Asit Ray:** Conceptualization, Supervision, Writing - review & editing.

Declaration of competing interest

The authors declare the following financial interests/personal relationships which may be considered as potential competing interests: No If there are other authors, they declare that they have no known competing financial interests or personal relationships that could have appeared to influence the work reported in this paper.

Acknowledgements

The authors are grateful to Dr. M. R. Nayak, President, Siksha 'O' Anusandhan (Deemed to be University) and Dr. S. C. Si, Dean, School of Pharmaceutical Sciences for providing necessary facilities for carrying out the research work.

Abbreviations

CZEO	Cinnamomum zeylanicum essential oil
GC-MS	Gas chromatography-mass spectrometry
ADME	Absorption, Distribution, Metabolism, Excretion
STP	Swiss Target Prediction
SEALAB	Similarity Ensemble Approach
OMIM	Online Mendelian Inheritance in Man
AI	Anti-inflammation
HBA	Hydrogen bond acceptor
HBD	Hydrogen bond donor
MLOGP	Moriguchi octanol-water partition coefficient
STRING	Search Tool for the Retrieval of Interacting Genes/Proteins
PPI	Protein Protein Interaction
GO	Gene Ontology
KEGG	Kyoto Encyclopaedia of Genes and Genomes
FDR	False Discovery Rate
MTT	3-(4,5-Dimethylthiazol-2-yl)-2,5-diphenyltetrazolium bromide
TNF- α	Tumor necrosis factor- α
TLR4	Toll-like receptor 4
IL6	Interleukin 6
IL8	Interleukin 8
NF κ B	Nuclear factor kappa B
STAT3	Signal Transducer and Activator of Transcription Factor 3
FBS	Fetal Bovine Serum
DMEM	Dulbecco's Modified Eagle Medium
LPS	Lipopolysaccharide
DMSO	Dimethyl sulfoxide
NO	Nitric oxide
PGE ₂	Prostaglandin E ₂
ELISA	Enzyme Linked Immunosorbent Assay
IL-1 β	Interleukin- 1 β
SOD	Super oxide dismutase
GSH	Glutathione
CAT	Catalase
GPx	Glutathione peroxidase
ROS	Reactive oxygen species
DCFH-DA	Dichloro-dihydro-fluorescein diacetate
JC-1	5,5,6,6'-tetrachloro-1,1',3,3' tetraethylbenzimi-dazolcarbocyanine iodide
EIA	Enzyme Immunoassay
PBS	Phosphate buffer saline
RT-qPCR	Reverse transcription quantitative polymerase chain reaction
I κ B	Inhibitor of κ B
MAPK	Mitogen activated protein kinase
JAK-STAT	Janus kinase - Signal transducers and activators of transcription

References

- [1] D. Furman, J. Campisi, E. Verdin, P. Carrera-Bastos, S. Targ, C. Franceschi, L. Ferrucci, D.W. Gilroy, A. Fasano, G.W. Miller, A.H. Miller, Chronic inflammation in the etiology of disease across the life span, *Nat. Med* 25 (2019) 1822–1832, <https://doi.org/10.1038/s41591-019-0675-0>.
- [2] G.W. Schmid-Schönbein, Analysis of inflammation, *Annu. Rev. Biomed. Eng.* 8 (2006) 93–151, <https://doi.org/10.1146/annurev.bioeng.8.061505.095708>.
- [3] A.A. El-Banna, R.S. Darwish, D.A. Ghareeb, A.M. Yassin, S.A. Abdulmalek, H.M. Dawood, Metabolic profiling of *Lantana camara* L. using UPLC-MS/MS and revealing its inflammation-related targets using network pharmacology-based and molecular docking analyses, *Sci. Rep.* 12 (2022), <https://doi.org/10.1038/s41598-022-19137-0>.
- [4] L.B. Williams, J.B. Koenig, B. Black, T.W.G. Gibson, S. Sharif, T.G. Koch, Equine allogeneic umbilical cord blood derived mesenchymal stromal cells reduce synovial fluid nucleated cell count and induce mild self-limiting inflammation when evaluated in an lipopolysaccharide induced synovitis model, *Equine Vet. J.* 48 (2016) 619–625, <https://doi.org/10.1111/evj.12477>.
- [5] F. Raucci, A.J. Iqbal, A. Saviano, P. Minosi, M. Piccolo, C. Irace, F. Caso, R. Scarpa, S. Pieretti, N. Mascolo, F. Maione, IL-17A neutralizing antibody regulates monosodium urate crystal-induced gouty inflammation, *Pharmacol. Res.* 147 (2019), <https://doi.org/10.1016/j.phrs.2019.104351>.
- [6] P. Chauhan, D. Shukla, D. Chattopadhyay, B. Saha, Redundant and regulatory roles for Toll-like receptors in Leishmania infection, *Clin. Exp. Immunol.* 190 (2017) 167–186, <https://doi.org/10.1111/cei.13014>.

- [7] N.Y. Kim, S. Kim, H.M. Park, C.M. Lim, J. Kim, J.Y. Park, K.B. Jeon, A. Poudel, H.P. Lee, S.R. Oh, J. Ahn, *Cinnamomum verum* extract inhibits NOX2/ROS and PKC δ /JNK/AP-1/NF- κ B pathway-mediated inflammatory response in PMA-stimulated THP-1 monocytes, *Phytomedicine* 112 (2023), <https://doi.org/10.1016/j.phymed.2023.154685>.
- [8] N. Fujiwara, K. Kobayashi, Macrophages in inflammation, *Inflamm. Allergy - Drug Targets* 4 (2005) 281–286, <https://doi.org/10.2174/1568010054022024>.
- [9] S. Jena, A. Ray, O. Mohanta, P.K. Das, A. Sahoo, S. Nayak, P.C. Panda, *Neocinnamomum caudatum* essential oil ameliorates lipopolysaccharide-induced inflammation and oxidative stress in RAW 264.7 cells by inhibiting NF- κ B activation and ROS production, *Molecules* 27 (2022), <https://doi.org/10.3390/molecules27238193>.
- [10] R.N. Raka, D. Zhiqian, Y. Yue, Q. Luchang, P. Suyeon, X. Junsong, W. Hua, *Pingyin rose* essential oil alleviates LPS-Induced inflammation in RAW 264.7 cells via the NF- κ B pathway: an integrated *in vitro* and network pharmacology analysis, *BMC Compl. Alternative Med.* 22 (2022) 1–16, <https://doi.org/10.1186/s12906-022-03748-1>.
- [11] M.A. Ajmone-Cat, A. Bernardo, A. Greco, L. Minghetti, Non-steroidal anti-inflammatory drugs and brain inflammation: effects on microglial functions, *Pharmaceuticals* 3 (2010) 1949–1965, <https://doi.org/10.3390/ph3061949>.
- [12] Q. Zhao, L. Zhu, S. Wang, Y. Gao, F. Jin, Molecular mechanism of the anti-inflammatory effects of plant essential oils: a systematic review, *J. Ethnopharmacol.* 14 (2022), <https://doi.org/10.1016/j.jep.2022.115829>.
- [13] T. Debnath, D.H. Kim, B.O. Lim, Natural products as a source of anti-inflammatory agents associated with inflammatory bowel disease, *Molecules* 18 (2013) 7253–7270, <https://doi.org/10.3390/molecules18067253>.
- [14] J. Wang, B. Su, H. Jiang, N. Cui, Z. Yu, Y. Yang, Y. Sun, Traditional uses, phytochemistry and pharmacological activities of the genus *Cinnamomum* (Lauraceae): a review, *Fitoterapia* 146 (2020).
- [15] P. Ranasinghe, S. Pigera, G.A. Premakumara, P. Galappaththy, G.R. Constantine, P. Katulanda, Medicinal properties of ‘true’ cinnamon (*Cinnamomum zeylanicum*): a systematic review, *BMC Compl. Alternative Med.* 13 (2013) 1–10, <http://www.biomedcentral.com/1472-6882/13/275>.
- [16] G.K. Jayaprakasha, L.J. Rao, K.K. Sakariah, Chemical composition of volatile oil from *Cinnamomum zeylanicum* buds, *Z. Naturforsch., C: J. Biosci.* 57 (2002) 990–993, <https://doi.org/10.1515/znc-2002-11-1206>.
- [17] M. Saleem, H.N. Bhatti, M.I. Jilani, M.A. Hanif, Bioanalytical evaluation of *Cinnamomum zeylanicum* essential oil, *Nat. Prod. Res.* 29 (2015) 1857–1859, <https://doi.org/10.1080/14786419.2014.1002088>.
- [18] X. Han, T.L. Parker, Antiinflammatory activity of Cinnamon (*Cinnamomum zeylanicum*) bark essential oil in a human skin disease model, *Phytother Res.* 31 (2017) 1034–1038, <https://doi.org/10.1002/ptr.5822>.
- [19] F. Esmaeili, M. Zahmatkeshan, Y. Yousefpoor, H. Alipanah, E. Safari, M. Osanloo, Anti-inflammatory and anti-nociceptive effects of Cinnamon and Clove essential oils nanogels: an *in vivo* study, *BMC Complement Med Ther* 22 (2022) 1–10, <https://doi.org/10.1186/s12906-022-03619-9>.
- [20] S.H. Shi, Y.P. Cai, X.J. Cai, X.Y. Zheng, D.S. Cao, F.Q. Ye, Z. Xiang, A network pharmacology approach to understanding the mechanisms of action of traditional medicine: bushenhuoxue formula for treatment of chronic kidney disease, *PLoS One* 9 (2014), <https://doi.org/10.1371/journal.pone.0089123>.
- [21] X. Lai, X. Wang, Y. Hu, S. Su, W. Li, S. Li, Network pharmacology and traditional medicine, *Front. Pharmacol.* 11 (2020), <https://doi.org/10.3389/fphar.2020.01194>.
- [22] *European Pharmacopoeia, seventh ed., Council of Europe, Strasbourg, 2011, pp. 1160–1161.*
- [23] R.P. Adams, *Identification of Essential Oil Components by Gas Chromatography/Mass Spectroscopy*, Allured Publishing Corporation: Carol Stream, IL, USA, 2007.
- [24] H. Di, H. Liu, S. Xu, N. Yi, G. Wei, Network pharmacology and experimental validation to explore the molecular mechanisms of compound Huangbai liquid for the treatment of acne, *Drug Des. Dev. Ther.* 17 (2023) 39–53, <https://doi.org/10.2147/DDDT.S385208>.
- [25] Q.D. Xia, Y. Xun, J.L. Lu, Y.C. Lu, Y.Y. Yang, P. Zhou, J. Hu, C. Li, S.G. Wang, Network pharmacology and molecular docking analyses on Lianhua Qingwen capsule indicate Akt 1 is a potential target to treat and prevent COVID-19, *Cell Prolif.* 53 (2020), <https://doi.org/10.1111/cpr.12949>.
- [26] T.H. Huang, N. Mokgautsi, Y.J. Huang, A.T. Wu, H.S. Huang, Comprehensive omics analysis of a novel small-molecule inhibitor of chemoresistant oncogenic signatures in colorectal cancer cell with antitumor effects, *Cells* 10 (2021) 1–21, <https://doi.org/10.3390/cells10081970>.
- [27] X. Sun, Q. Xu, L. Zeng, L. Xie, Q. Zhao, H. Xu, X. Wang, N. Jiang, P. Fu, M. Sang, Resveratrol suppresses the growth and metastatic potential of cervical cancer by inhibiting STAT3/Tyr705 phosphorylation, *Cancer Med.* 9 (2020) 8685–8700, <https://doi.org/10.1002/cam4.3510>.
- [28] I. Tabas, C.K. Glass, Anti-inflammatory therapy in chronic disease: challenges and opportunities, *Science* 339 (2013) 166–172, <https://doi.org/10.1126/science.1230720>.
- [29] A.B. Kunnumakkara, B.L. Sailo, K. Banik, C. Harsha, S. Prasad, S.C. Gupta, A.C. Bharti, B.B. Aggarwal, Chronic diseases, inflammation, and spices: how are they linked? *J. Transl. Med.* 16 (2018) 1–25, <https://doi.org/10.1186/s12967-018-1381-2>.
- [30] R. Lee, M.J. Balick, *Sweet wood-cinnamon and its importance as a spice and medicine*, *Explore* 1 (2005) 61–64.
- [31] R. Gogoi, N. Sarma, R. Loying, S.K. Pandey, T. Begum, M. Lal, A comparative analysis of bark and leaf essential oil and their chemical composition, antioxidant, anti-inflammatory, antimicrobial activities and genotoxicity of North East Indian *Cinnamomum zeylanicum* Blume, *Nat. Prod. Res.* 11 (2021) 74–84, <https://doi.org/10.2174/221031550966619111911800>.
- [32] L.K. Chao, K.F. Hua, H.Y. Hsu, S.S. Cheng, I.F. Lin, C.J. Chen, S.T. Chen, S.T. Chang, Cinnamaldehyde inhibits pro-inflammatory cytokines secretion from monocytes/macrophages through suppression of intracellular signalling, *Food Chem. Toxicol.* 46 (2008) 220–231, <https://doi.org/10.1016/j.fct.2007.07.016>.
- [33] Y.T. Tung, M.T. Chua, S.Y. Wang, S.T. Chang, Anti-inflammation activities of essential oil and its constituents from indigenous cinnamon (*Cinnamomum osmophloeum*) twigs, *Bioresour. Technol.* 99 (2008) 3908–3913, <https://doi.org/10.1016/j.biortech.2007.07.050>.
- [34] Y.K. Choi, G.S. Cho, S. Hwang, B.W. Kim, J.H. Lim, J.C. Lee, H.C. Kim, W.K. Kim, Y.S. Kim, Methyl Eugenol reduces cerebral ischemic injury by suppression of oxidative injury and inflammation, *Free Radic. Res.* 44 (2010) 925–935, <https://doi.org/10.3109/10715762.2010.490837>.
- [35] P. Chen, J. Zhou, A. Ruan, L. Zeng, J. Liu, Q. Wang, Cinnamic Aldehyde, the main monomer component of Cinnamon, exhibits anti-inflammatory property in OA synovial fibroblasts via TLR4/MyD88 pathway, *J. Cell Mol. Med.* 26 (2022) 913–924, <https://doi.org/10.1111/jcmm.17148>.
- [36] D. Gunawardena, N. Karunaweera, S. Lee, F. van Der Kooy, D.G. Harman, R. Raju, L. Bennett, E. Gyengesi, N.J. Sucher, G. Münch, Anti-inflammatory activity of cinnamon (*C. zeylanicum* and *C. cassia*) extracts—identification of E-cinnamaldehyde and o-methoxy cinnamaldehyde as the most potent bioactive compounds, *Food Funct.* 6 (2015) 910–919.
- [37] M. Adnan, A. Shamsi, A.M. Elasbali, A.J. Siddiqui, M. Patel, N. Alshammari, S.H. Alharethi, H.H. Alhassan, F. Bardakci, M.I. Hassan, Structure-guided approach to discover Tuberosin as a potent activator of pyruvate kinase M2, targeting cancer therapy, *Int. J. Mol. Sci.* 23 (2022), <https://doi.org/10.3390/ijms232113172>.
- [38] S. Jacob, M.A. VanDaele, J.N. Brown, Treatment of Demodex-associated inflammatory skin conditions: a systematic review, *Dermatol. Ther.* 32 (2019), <https://doi.org/10.1111/dth.13103>.
- [39] F.M.N. Forton, V. De Maertelaer, Treatment of rosacea and demodicosis with benzyl benzoate: effects of different doses on demodex density and clinical symptoms, *J. Eur. Acad. Dermatol. Venereol.* 34 (2020) 365–369, <https://doi.org/10.1111/jdv.15938>.
- [40] I. Komala, N. Supandi, O.S. Betha, E. Putri, S. Mufidah, M.F. Awaludin, M. Fahmi, M. Reza, N.P. Indriyani, Structure-activity relationship study on the ethyl p-methoxycinnamate as an anti-inflammatory agent, *Indones. J. Chem.* 18 (2018) 60–65, <https://doi.org/10.22146/ijc.26162>.
- [41] Y.H. Kang, J.S. Kang, H.M. Shin, Vasodilatory effects of cinnamic acid via the nitric oxide-cGMP-PKG pathway in rat thoracic aorta, *Phytother Res.* 27 (2013) 205–211.
- [42] D.L. Compton, J.A. Laszlo, M.A. Berhow, Lipase-catalyzed synthesis of ferulate esters, *J. Am. Oil Chem. Soc.* 77 (2000) 513–519, <https://doi.org/10.1007/s11746-000-0082-9>.
- [43] M. DellaGreca, L. Previtera, R. Purcaro, A. Zarrelli, Cinnamic ester derivatives from *Oxalis pes-caprae* (*Bermuda buttercup*), *J. Nat. Prod.* 70 (2007) 1664–1667, <https://doi.org/10.1021/np0702786>.
- [44] V. Aparna, K.V. Dileep, P.K. Mandal, P. Karthe, C. Sadasivan, M. Haridas, Anti-inflammatory property of n-hexadecanoic acid: structural evidence and kinetic assessment, *Chem. Biol. Drug Des.* 80 (2012) 434–439, <https://doi.org/10.1111/j.1747-0285.2012.01418.x>.

- [45] G.S. Ashcroft, M.J. Jeong, J.J. Ashworth, M. Hardman, W. Jin, N. Moutsopoulos, T. Wild, N. McCartney-Francis, D. Sim, G. McGrady, X.Y. Song, Tumor necrosis factor- α (TNF- α) is a therapeutic target for impaired cutaneous wound healing, *Wound Repair Regen.* 20 (2012) 38–49, <https://doi.org/10.1111/j.1524-475X.2011.00748.x>.
- [46] B. Salvador, A. Arranz, S. Francisco, L. Cordoba, C. Punzon, M.Á. Llamas, M. Fresno, Modulation of endothelial function by Toll like receptors, *Pharmacol. Res.* 108 (2016) 46–56, <https://doi.org/10.1016/j.phrs.2016.03.038>.
- [47] C. Gabay, Interleukin-6 and chronic inflammation, *Arthritis Res. Ther.* 2 (2006) 1–6, <https://doi.org/10.1186/ar1917>.
- [48] J.E. Pease, I. Sabroe, The role of interleukin-8 and its receptors in inflammatory lung disease: implications for therapy, *Am. J. Respir. Med.* 1 (2002) 19–25.
- [49] M.M. Kasembeli, U. Bharadwaj, P. Robinson, D.J. Tweardy, Contribution of STAT3 to inflammatory and fibrotic diseases and prospects for its targeting for treatment, *Int. J. Mol. Sci.* 19 (2018), <https://doi.org/10.3390/ijms19082299>.
- [50] T. Lawrence, The nuclear factor NF- κ B pathway in inflammation, *Cold Spring Harbor Perspect. Biol.* 1 (2009), <https://doi.org/10.1101/cshperspect.a001651>.
- [51] J.S. Yu, J. Jin, Y.Y. Li, The physiological functions of IKK-selective substrate identification and their critical roles in diseases, *STEMedicine* 1 (2020), <https://doi.org/10.37175/stemedicine.v1i4.49>.
- [52] K. Adelman, M.A. Kennedy, S. Nechaev, D.A. Gilchrist, G.W. Muse, Y. Chinenov, I. Rogatsky, Immediate mediators of the inflammatory response are poised for gene activation through RNA polymerase II stalling, *Proc. Natl. Acad. Sci.* 106 (2009) 18207–18212, <https://doi.org/10.1073/pnas.0910177106>.
- [53] S.W. Tas, P.H. Remans, K.A. Reedquist, P.P. Tak, Signal transduction pathways and transcription factors as therapeutic targets in inflammatory disease: towards innovative antirheumatic therapy, *Curr. Pharm. Des.* 11 (2005) 581–611, <https://doi.org/10.2174/1381612053381918>.
- [54] M. Chen, Y.Y. Chang, S. Huang, L.H. Xiao, W. Zhou, L.Y. Zhang, C. Li, R.P. Zhou, J. Tang, L. Lin, Z.Y. Du, Aromatic-Turmerone attenuates LPS-Induced neuroinflammation and consequent memory impairment by targeting TLR4-Dependent signalling pathway, *Mol. Nutr. Food Res.* 62 (2018), <https://doi.org/10.1002/mnfr.201700281>.
- [55] J. Liao, X. Xie, W. Wang, Y. Gao, Y. Cai, J. Peng, T. Li, Q. Yi, C. He, L. Wang, Anti-inflammatory activity of essential oil from leaves of *Blumea balsamifera* (L.) DC through inhibiting TLR4/NF- κ B signaling pathways and NLRP3 inflammasome activation in LPS-induced RAW 264.7 macrophage cells, *J. Essent. Oil-Bear Plants* 24 (2021) 160–176, <https://doi.org/10.1080/0972060X.2021.1912645>.
- [56] S.S. Arango-Varela, I. Luzardo-Ocampo, M.E. Maldonado-Celis, R. Campos-Vega, Andean berry (*Vaccinium meridionale* Swartz) juice in combination with aspirin modulated anti-inflammatory markers on LPS-stimulated RAW 264.7 macrophages, *Food Res. Int.* 137 (2020), <https://doi.org/10.1016/j.foodres.2020.109541>.
- [57] M. Nakanishi, D.W. Rosenberg, Multifaceted roles of PGE 2 in inflammation and cancer, *Semin. Immunopathol.* 35 (2013) 123–137, <https://doi.org/10.1007/s00281-012-0342-8>.
- [58] S. Xiao, H. Yu, Y. Xie, Y. Guo, J. Fan, W. Yao, The anti-inflammatory potential of *Cinnamomum camphora* (L.) J. Presl essential oil *in vitro* and *in vivo*, *J. Ethnopharmacol.* 267 (2021), <https://doi.org/10.1016/j.jep.2020.113516>.
- [59] C.T. Lin, C.J. Chen, T.Y. Lin, J.C. Tung, S.Y. Wang, Anti-inflammation activity of fruit essential oil from *Cinnamomum insularimontanum* Hayata, *Bioresour. Technol.* 99 (2008) 8783–8787, <https://doi.org/10.1016/j.biortech.2008.04.041>.
- [60] J. Tang, P. Diao, X. Shu, L. Li, L. Xiong, Quercetin and quercitrin attenuates the inflammatory response and oxidative stress in LPS-induced RAW264. 7 cells: *in vitro* assessment and a theoretical model, *BioMed Res. Int.* (2019), <https://doi.org/10.1155/2019/7039802>.
- [61] D.W. Seo, Y.J. Yi, M.S. Lee, B.S. Yun, S.M. Lee, Differential modulation of lipopolysaccharide-induced inflammatory cytokine production by and antioxidant activity of fomentariol in RAW 264.7 cells, *MYCOBIOLOGY* 43 (2015) 450–457, <https://doi.org/10.5941/MYCO.2015.43.4.450>.
- [62] P.K. Mittal, M. Anand, A.K. Madan, S. Yadav, J. Kumar, Antioxidative capacity of vitamin E, vitamin C and their combination in cryopreserved Bhadavari bull semen, *Vet. World* 7 (2014) 1127–1131, <https://doi.org/10.14202/vetworld.2014.1127-1131>.
- [63] M. Sharifi-Rad, N.V. Anil Kumar, P. Zucca, E.M. Varoni, L. Dini, E. Panzarini, J. Rajkovic, P.V. Tsouh Fokou, E. Azzini, I. Peluso, A. Prakash Mishra, Lifestyle, oxidative stress, and antioxidants: back and forth in the pathophysiology of chronic diseases, *Front. Physiol.* 11 (2020), <https://doi.org/10.3389/fphys.2020.00694>.
- [64] I.L.C. Chapple, Reactive oxygen species and antioxidants in inflammatory diseases, *J. Clin. Periodontol.* 24 (1997) 287–296.
- [65] T.Q. Nguyen, T. Duy Binh, T.L. Pham, Y.D. Nguyen, D. Thi Xuan Trang, T.T. Nguyen, K. Kanaori, K. Kamei, Anti-inflammatory effects of *Lasia spinosa* leaf extract in lipopolysaccharide-induced RAW 264.7 macrophages, *Int. J. Mol. Sci.* 21 (2020), <https://doi.org/10.3390/ijms21103439>.
- [66] P. Wan, M. Xie, G. Chen, Z. Dai, B. Hu, X. Zeng, Y. Sun, Anti-inflammatory effects of dicaffeoylquinic acids from *Ilex kudingcha* on lipopolysaccharide-treated RAW 264. 7 macrophages and potential mechanisms, *Food Chem. Toxicol.* 126 (2019) 332–342.
- [67] X. Hao, W. Sun, C. Ke, F. Wang, Y. Xue, Z. Luo, X. Wang, J. Zhang, Y. Zhang, Anti-inflammatory activities of leaf oil from *Cinnamomum subavenium* *in vitro* and *in vivo*, *BioMed Res. Int.* (2019), <https://doi.org/10.1155/2019/1823149>.